

Department of Neurology  
Faculty M: Medicine  
Saarland University, Homburg/Saar, Germany

**ACID SPHINGOMYELINASE DEFICIENCY  
BLOCKS CHRONIC EXPERIMENTAL AUTOIMMUNE ENCEPHA-  
LOMYELITIS AND IMPROVES MYELIN REPAIR**

**Dissertation**

*A dissertation submitted in fulfillment of the requirements for the  
degree of Doktors der Naturwissenschaften  
(Dr. rer. nat.)*

Faculty of Medicine  
SAARLAND UNIVERSITY  
2017

**Submitted by: Marwan Chami**  
Born on: 22 September 1986, in Orosháza, Hungary

***To my mother (1962-2007)***

***Without her I wouldn't be where I am today***

## **Declaration**

I hereby declare that this thesis is my own original work and effort. All experiments, except for those specified, were exclusively performed by me. Except for the publications written by myself listed in the publication list, the data presented here have not been submitted anywhere else for any award. Where other sources of information and help have been used, they have been indicated and acknowledged.

Homburg/Saar

**I Contents**

Abstract ..... 5

Zusammenfassung..... 7

1. Introduction..... 9

    1.1 Multiple Sclerosis: overview..... 9

    1.2 MS epidemiology ..... 9

    1.3 MS etiology ..... 10

    1.4 MS pathophysiology..... 10

    1.5 Animal models of MS ..... 12

    1.6 Available treatments for MS..... 14

    1.7 T cells and glia in MS..... 15

    1.8 Sphingolipids and Acid Sphingomyelinase ..... 20

        1.8.1 Sphingolipids in MS and de/remyelination ..... 22

2 Aim of work..... 25

3 Materials and methods ..... 26

    3.1 Materials ..... 26

        3.1.1 Instruments..... 26

        3.1.2 Experimental material..... 27

        3.1.3 Chemicals..... 28

        3.1.4 Kits..... 29

        3.1.5 Oligonucleotides ..... 29

        3.1.6 Antibodies..... 29

        3.1.7 Buffers and media ..... 30

    3.2 Methods ..... 30

        3.2.1 Mice ..... 30

        3.2.2 Immunization, clinical scoring guide and treatment protocols..... 31

        3.2.3 Induction of experimental de- and remyelination, treatment groups and amitriptyline treatment..... 33

    3.3 Tissue collection ..... 34

    3.4 Histology ..... 35

        3.4.1 Luxol Fast Blue Stain (LFB) ..... 35

    3.5 Immunohistochemistry ..... 36

        3.5.1 GFAP, Iba-1, CD3, Olig-2, synaptophysin and APP staining..... 36

        3.5.2 MBP fluorescence staining..... 38

    3.6 Quantification of de- and remyelination ..... 38

    3.7 Quantification of inflammation and lesions in spinal cords of chEAE mice ..... 39

    3.8 Quantification of oligodendrocyte and T-cell numbers ..... 40

    3.9 Quantification of astrocyte and microglia parameters ..... 41

    3.10 MBP fluorescence quantification ..... 41

    3.11 Reverse transcription and quantitative PCR for analysis of gene transcripts..... 42

        3.11.1 Corpus callosum RNA isolation with Trizol ..... 42

        3.11.2 Genome DNA degradation prior to RT-PCR ..... 44

3.11.3	First strand cDNA synthesis .....	44
3.11.4	Real-time quantitative PCR .....	45
3.12	Statistics .....	46
4	Results .....	47
4.1	Smpd1 deficiency prevents chEAE symptoms and demyelination .....	47
4.2	T cell infiltration to the CNS is inhibited by Smpd1 deficiency .....	48
4.3	Smpd1 deficiency significantly decreases astrogliosis and microgliosis .....	49
4.4	Pharmacological inhibition of ASM by amitriptyline attenuates chEAE symptoms, astrogliosis and microgliosis .....	51
4.5	Smpd1 deficiency enhances myelin recovery after acute and chronic demyelination .....	54
4.6	Smpd1 deficiency reduces astrogliosis and production of inflammatory cytokines after acute demyelination .....	57
4.7	Pharmacological inhibition of ASM as therapeutic option for myelin repair .....	59
5	Discussion .....	63
5.1	Acid sphingomyelinase deficiency in chEAE pathophysiology .....	64
5.2	Pharmacological inhibition of ASM in chEAE .....	65
5.3	Acid sphingomyelinase deficiency in de- and remyelination .....	66
5.4	Pharmacological inhibition of acid sphingomyelinase and myelin repair .....	68
6	References .....	71
7	Publications .....	79
8	Acknowledgements .....	80
9	Curriculum Vitae .....	<b>Error! Bookmark not defined.</b>
	Figures .....	81
	Abbreviations .....	82

### **Abstract**

Multiple sclerosis is an immune mediated disease effecting the central nervous system, characterized by inflammatory infiltrates, axonal loss, demyelination and plaque formation. The invasion of the central nervous system by inflammatory auto-reactive lymphocytes leads to an inflammatory effector phase. Multiple sclerosis is documented as a major cause of neurological disability in young populations affecting more than 2.5 million people around the world. Still to date, the cause of multiple sclerosis is not yet fully elucidated, considerable knowledge about its pathophysiology has been studied. In addition to that, there's no cure present for this devastating condition despite the availability of several disease-modifying treatments. These drugs have been reported to reduce the number of relapses, but unfortunately none of these treatments can completely protect against disease progression. Adding to that, many of the disease-modifying therapies used to treat multiple sclerosis hold major health risks, such as cardiotoxicity, liver damage and progressive multifocal leukoencephalopathy. Therefore, identification of novel targets and the development of new therapeutic options are crucial steps for the treatment of multiple sclerosis patients.

In this study, we investigated the role of the acid sphingomyelinase/ceramide pathway in two animal models of multiple sclerosis. Using the chronic experimental autoimmune encephalomyelitis model we demonstrate that both genetic deficiency and the pharmacological inhibition of acid sphingomyelinase by amitriptyline inhibit the infiltration of lymphocytes to the central nervous system and abolish clinical symptoms, with a decreased astrogliosis and microgliosis. Sphingolipids, in particular ceramide, and the enzyme acid sphingomyelinase,

which generates ceramide from sphingomyelin, seem to be involved in lymphocyte infiltration to the central nervous system.

The second model, the toxic demyelination model or as called the cuprizone model was employed to study central nervous demyelination without the direct immunological influence observed in the experimental autoimmune encephalomyelitis model. We demonstrate that mice lacking the enzyme acid sphingomyelinase show a significantly higher/faster myelin recovery after acute or chronic myelin damage by enhancement of oligodendrocyte proliferation, decreased astroglial activation and axonal damage. Inhibition of acid sphingomyelinase using the drug amitriptyline mimicked the genetic deficiency effects and may constitute a novel therapeutic approach to prevent chronic degeneration in multiple sclerosis.

## Zusammenfassung

Multiple Sklerose ist eine chronisch entzündliche Erkrankung des zentralen Nervensystems, gekennzeichnet durch entzündliche Infiltrate, axonalen Verlust, Demyelinisierung und Plaquebildung. Die Invasion des Zentralnervensystems durch entzündliche autoreaktive Lymphozyten führt zu einer Kaskade entzündlicher Reaktionen. Multiple Sklerose ist die häufigste Ursache für neurologische Behinderung bei jungen Erwachsenen mit mehr als 2,5 Millionen Menschen weltweit. Noch immer ist die Ursache der Multiplen Sklerose trotz umfangreichem Wissen über ihre Pathophysiologie noch nicht vollständig aufgeklärt. Darüber hinaus gibt es zum heutigen Zeitpunkt keine Heilung für Multiple Sklerose, trotz der Verfügbarkeit von mehreren krankheitsverändernde Behandlungen, einschließlich Interferonen, Mitoxantron und FTY720. Diese Medikamente haben gezeigt, dass die Anzahl der Schübe reduzierbar ist, aber leider können keine dieser Behandlungen vollständig vor dem Fortschreiten der Krankheit schützen. Hinzu kommt, dass viele der krankheitsmodifizierenden Therapien, die zur Behandlung von Multipler Sklerose eingesetzt werden, erhebliche Gesundheitsrisiken wie Kardiotoxizität, Leberschädigung und progressive multifokale Leukoenzephalopathie mit sich bringen können. Daher sind die Identifizierung neuer Ziele und die Entwicklung neuer Therapieoptionen entscheidende Schritte zur Behandlung von Patienten mit Multipler Sklerose.

In dieser Studie untersuchten wir die Rolle des sauren Sphingomyelinase / Ceramid Systems in zwei Tiermodellen der Multiple Sklerose. Unter Verwendung des chronischen experimentellen Autoimmun-Enzephalomyelitis-Modells zeigten wir, dass sowohl der genetische Mangel als auch die

pharmakologische Hemmung der sauren Sphingomyelinase durch Amitriptylin die Infiltration von Lymphozyten in das zentrale Nervensystem hemmen und die klinischen Symptome mit einer verminderten Astrogliose und Mikrogliose beseitigen kann. Sphingolipide, insbesondere Ceramide, und das Enzym saure Sphingomyelinase, das Ceramid aus Sphingomyelin erzeugen kann, und Infiltration von Lymphozyten in das zentrale Nervensystem beteiligt zu sein. Diese Ergebnisse entsprechen früheren Berichten, die die Beziehung von Ceramid-angereicherten Membranplattformen bei der Signalamplifikation und neuronaler Schädigung bei Multipler Sklerose zeigen.

Das zweite Modell, das toxische Demyelinisierung Modell oder das sogenannte Cuprizinmodell, wurde verwendet, um die zentrale nervöse Demyelinisierung ohne den direkten immunologischen Einfluss zu untersuchen, der in dem experimentellen Autoimmun-Enzephalomyelitis-Modell beobachtet wurde. Wir zeigen, dass Mäuse, denen die saure Sphingomyelinase fehlt, nach einer akuten oder chronischen Myelinschädigung durch Verstärkung der Oligodendrozytenproliferation, verminderter astroglialer Aktivierung und axonaler Schädigung einen signifikanten Anstieg der Remyelinisierung zeigen. Die Hemmung der sauren Sphingomyelinase unter Verwendung des Medikaments Amitriptylin imitiert die Auswirkung des genetischen Mangels und kann einen neuen therapeutischen Ansatz darstellen, um eine chronische Degeneration bei Multipler Sklerose zu verhindern.

## 1. Introduction

### 1.1 Multiple Sclerosis: overview

Multiple Sclerosis (MS) is a demyelinating disease which is often described as an autoimmune disease of the central nervous system (CNS). Unfolded initially in 1838, today MS is recognized worldwide affecting more than 2.5 million individuals. With its wide distribution, MS is widely spread among young adults worldwide causing major neurological disabilities. It is documented that MS is affecting women more often than men (Sospedra and Martin 2005; Pugliatti et al., 2006). MS is categorized into four subtypes; relapsing-remitting (RR), secondary-progressive (SP), primary-progressive (PP), and progressive-relapsing (PR) – according to the clinical course of the disease (Lubin and Reingold, 1996). Most MS patients have a relapsing-remitting (RRMS) subtype, where a full recovery between relapses could be observed. But with time these patients do not recover fully between relapses and develop a secondary-progressive (SP) form of MS (Compston et al., 2006). The less common form of MS which 15% of patients develop is a primary-progressive (PPMS) characterized by a continuous worsening in neurological functions (Lubin et al., 1996; Miller et al., 2007). Today the diagnosis of MS is based on clinical symptoms and MRI features, which physicians evaluate using an evolving set of criteria, called the McDonald Criteria (Polman et al., 2011).

### 1.2 MS epidemiology

The diagnosis of MS has increased with a 0.7-8.7 per 100,000/year and a prevalence of 1-287 per 100,000 people (Rosati, 2001). MS distribution varies with geographic latitude <5 cases per 100,000 people in Asia and >100-200 cases

per 100,000 people including northern Europe. Also, as mentioned by Charcot and others the prevalence of females with MS worldwide is double as of males with a ratio 2:1, specifically Canada where the female/male ratio is 3:1 (Compton et al., 2006).

### **1.3 MS etiology**

The etiology of MS is still unknown to this date, but most of the research done is pointing toward the involvement of three major factors. The genetic vulnerability, several studies are being carried out in an effort to identify associated risk and susceptibility genes, protection and disease severity genes (Haines et al., 1996). Environmental exposures are considered as a second factor; both vitamin D deficiency and Epstein-Barr virus (EBV) infection have been related to MS development. The third factor is the host immune system, attacking and destroying the CNS, hence MS is considered as an autoimmune disease (Barnett et al., 2009; Syed and Rizvi et al., 2011).

### **1.4 MS pathophysiology**

Histopathological hallmarks of MS consist of inflammatory plaques with the infiltration of T cells, B cells, and macrophages, glial scar formation, loss of oligodendrocytes, myelin break down, and axonal damage/loss, which is the major factor causing irreversible damage in patients with MS (Lassmann et al., 2001). In MS several events are well documented such as; the breakdown of the blood-brain barrier (BBB), infiltration of T cells attacking the myelin leading to axonal damage, formation of lesions referred to as plaques accompanied with focal inflammation as shown in figure one.

Recovery and remyelination is a highly complex process. The formation of glial scars consisting of reactive astrocytes can be observed, which in turn prevents in most cases a normal remyelination process. Astrocytes are documented to activate microglia indirectly to engulf myelin debris. To make a way for new oligodendrocyte precursor cells to remyelinate the damaged area. Therefore, astrocytes are reported to play a dual role in de- and remyelination (Trap et al., 2008; Syed and Rizvi., 2011).

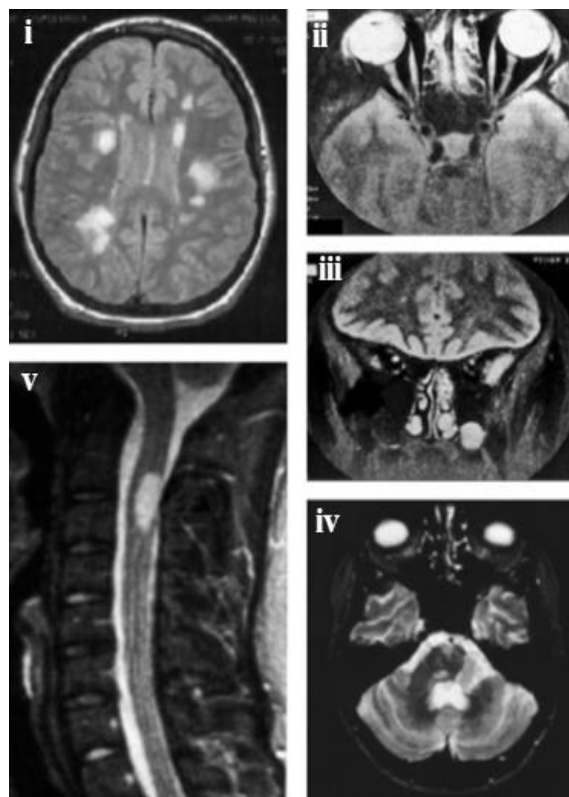


**Figure 1: MRI abnormalities in relapsing–remitting multiple sclerosis. Scars can be detected affecting the cerebrum (i), optic nerve (ii), (iii) cerebellar peduncle (iv), and spinal cord (v) (Compston et al., 2006).**

The phagocytosis of myelin is primarily not a CD4+ T cell mediated process; it represents the macrophage's natural response to injury (Henderson et al., 2009). On the other hand, CD4+ and CD8+ T cells are distributed along demyelinated tissues, with B cells and, occasionally regenerating oligodendrocytes.

Active plaques are characterized by the presence of partly demyelinated axons and macrophages filled with myelin debris (Prineas et al., 2002). Plaques pathology involves edema and inflammation, myelin loss, oligodendrocyte apoptosis, astrocyte and microglia activation which in turn results in the releasing of several chemokines and cytokines such as interleukin-1 (IL-1); IL-2; tumor necrosis factor (TNF); interferon- $\gamma$  (IFN $\gamma$ ). With time cells are cleared and a permanent area of damage surrounded by an astrocytic scar appears (Syed and Rizvi et al., 2011).

### **1.5 Animal models of MS**

Experimental Autoimmune Encephalomyelitis (EAE), which was developed in 1933 (Rivers et al., 1933) it is one of the widely used models. It is achieved by immunizing with myelin oligodendrocyte glycoprotein (MOG), myelin basic protein (MBP), or proteolipid protein (PLP). In EAE, CD4+ and CD8+ T cells and humoral immune responses play a role. MOG-induced EAE perhaps mimics the most of what we see in MS patients, however, no EAE model could one hundred percent duplicate MS.

For de- and remyelination several animal models exist; genetic myelin mutation, EAE, viral induced demyelination (e.g. Theiler's Murine Encephalomyelitis virus, TMEV) an infectious animal model, causing a polioencephalomyelitis in mice, followed by an inflammatory demyelinating spinal cord infection (Sato et al., 2010; Gudi 2010), and toxically induced demyelination (e.g. cuprizone, ethidium bromide, or lysolecithin), as demonstrated in figure 2. All these models mimic only a part of MS pathology (Olitsky and Yager, 1949; Gold et al., 2000; Gudi 2010).

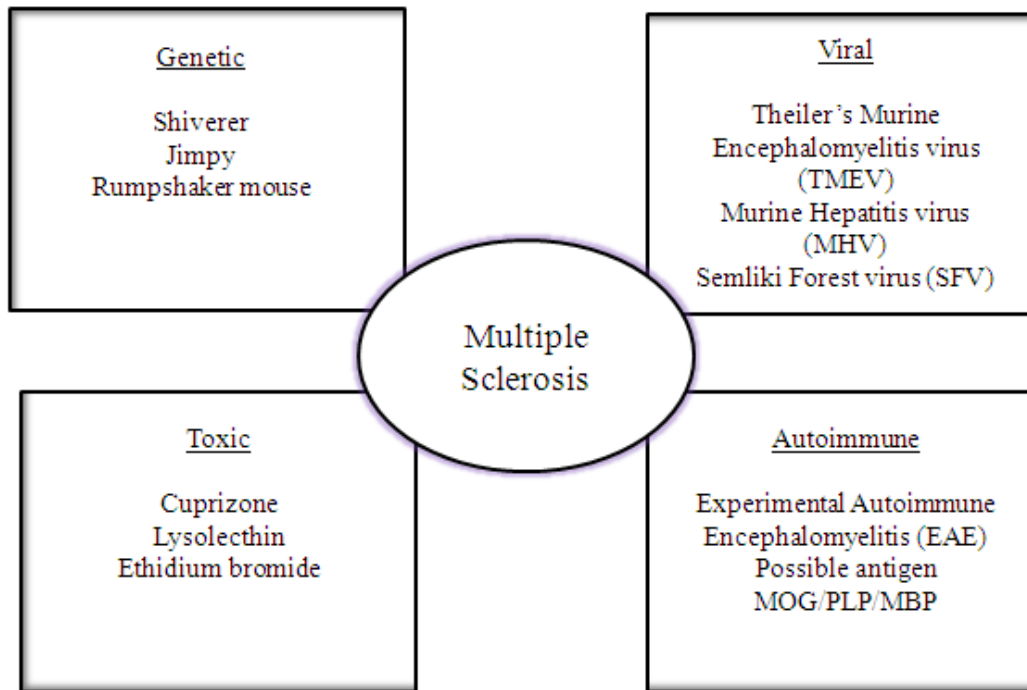


**Figure 2: Experimental animal models of MS. Different animal models of MS used for different research purposes.**

The cuprizone model is a widely used model. Mice are fed with the copper chelator cuprizone (bis-cyclohexanone oxaldihydrazone) for several weeks leading to a loss of oligodendrocytes and a subsequent demyelination accompanied by microgliosis and astrogliosis. After withdrawal of the toxin, remyelination occurs within weeks (Hiremath et al., 1998; Matsushima and Morell, 2001).

Using the cuprizone model, the BBB stays intact (Bakker and Ludwin, 1987) and de-remyelination can be analyzed without infiltration of T cells and peripheral macrophages. The extent of de- and remyelination is strongly influenced by mouse age, gender, strain and the dose of cuprizone used (Matsushima and Morell, 2001; Ludwin, 1980; Armstrong et al., 2002; Blakemore, 1972). The cuprizone model has already been used for decades (Ludwin, 1978; Gudi 2010).

### 1.6 Available treatments for MS

Up to date, there is no cure for MS. Treatments focuses on accelerating the recovery from attacks, slowing the progression of the disease and managing the symptoms. For example, corticosteroids are being used for acute intervention, it has been shown to increase the speed of recovery after relapses. Corticosteroids have potent anti-inflammatory and immunosuppressive properties. Beta interferons-1a and -1b, are the most commonly used medication for MS. Interferon beta achieves an equilibrium of pro- and anti-inflammatory agents in the brain, decreasing the number of inflammatory cells crossing the BBB. Interferon beta therapy leads to a reduction of neuroinflammation.

Treatments that inhibit immune cell trafficking include Natalizumab and Fingolimod, both treatments work by inhibiting the entry of T cells to the CNS. Another approach is being applied to promote immune cell depletion.

Treatments for this approach include Alemtuzumab and Rituximab. Alemtuzumab (Lemtrada), decreases relapses by targeting a protein on the surface of immune cells causing a depletion in T cells. This can decrease the damage caused to nerve cells by the attacking immune cells. Several treatments were investigated in an effort to influence immune cells including dimethyl fumarate and Laquinimod. Dimethyl fumarate was reported achieving a significant positive result concerning relapse rate and progression in phase III clinical trial. And it was recommended for approval in the European Union in 2013 as an MS therapy. Both treatments have shown reduced relapses in patients with MS.

Other treatments are also used that works on inhibiting immune cell replication such as Mitoxantrone and Teriflunomide. Mitoxantrone (Novantrone), an immunomodulatory drug. Which is suggested that effects and works as an immunomodulatory substance, still the mechanism behind is not fully reported. Teriflunomide (Aubagio) stops and inhibits immune cells mitosis (including T- and B-cells) that attack and damage the CNS.

Different treatments are also available for MS signs and symptoms including, physical therapy, muscle relaxants and medications to reduce fatigue. Also different medications could be advised for depression, pain, sexual dysfunction, bladder or bowel control problems that are associated with MS (Mayo Foundation for Medical Education and Research, 2014).

### **1.7 T cells and glia in MS**

T cells play an important role in MS, thus considered by many an immune mediated disease. Therefore, T cells have been a major research focus. CD8+ T cells can be observed within MS lesions at all disease stages, significantly outnumbering CD4+ cells. CD8+ cells work as cytotoxic cells, activated in the periphery and invading the brain or spinal cord. Memory CD8+ cells are found in high numbers in blood and CSF of MS patients (Correale et al., 2010). CD8+ T cells are associated with axonal injury in early MS (Barnett et al., 2009). CD4+ Th1-like cells encourage pro-inflammatory cytokines and stimulate cellular immunity, while CD4+ Th2-like cells aid cytokines and contribute to humoral immunity. CD4+ T cells, naïve or activated, were reported to have abnormalities in number and/or function in MS patients vs. controls (Peterson et al., 2014). The most widely used animal model to study T cells in MS is the experimental

autoimmune encephalomyelitis (EAE) model, but still these models do not mimic all aspects of the disease.

In neuroinflammation or demyelination astrocytes are stimulated and astrogliosis can be observed leading to the release of free radical nitric oxide (NO), known to be toxic to neurons and oligodendrocytes and may induce neurodegeneration (Brown, 2007).

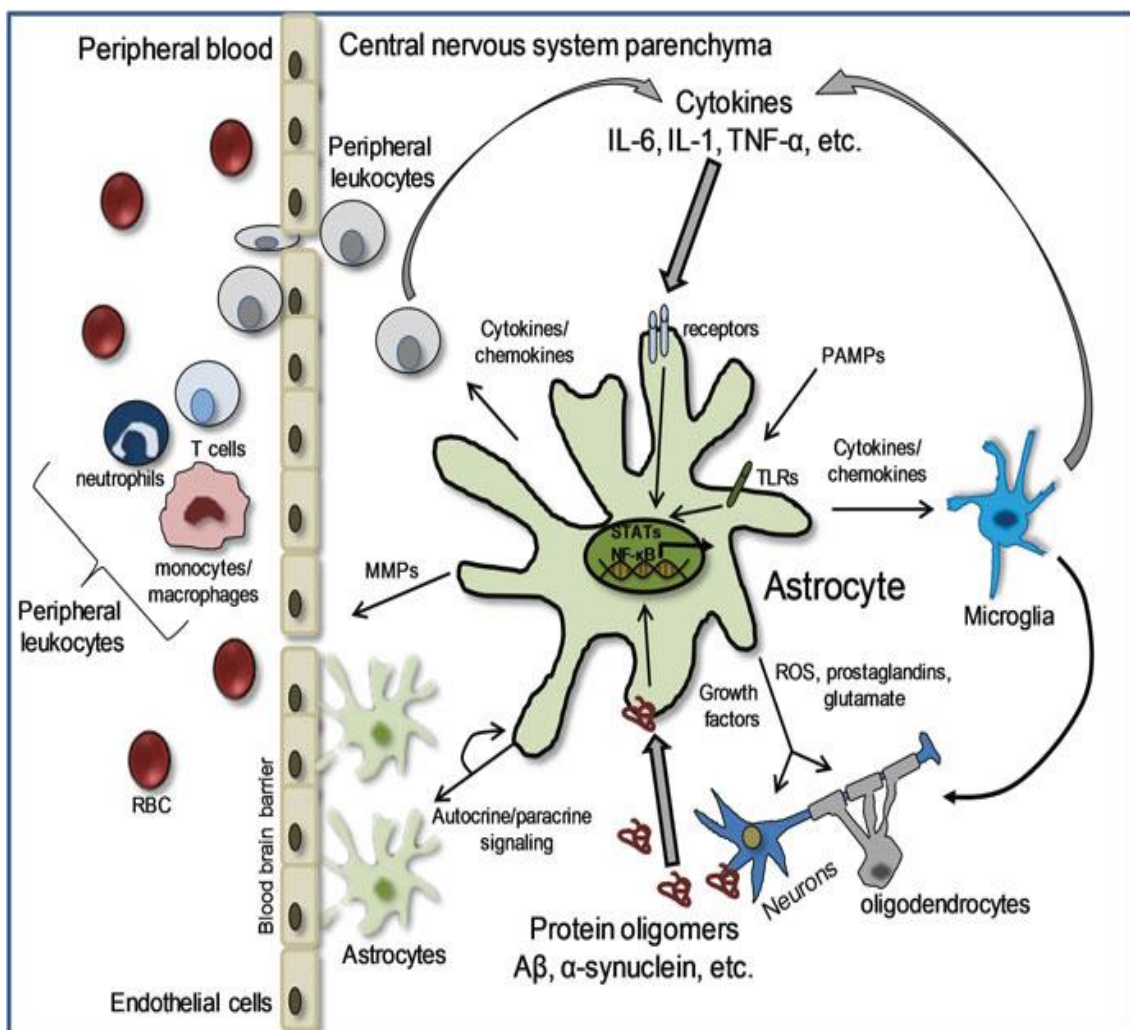


**Figure 2: Astrocytes orchestrate CNS inflammation (Peterson et al., 2014).**

In chronic cases like neurodegenerative diseases, astrocytes could play a role in pathophysiology, demonstrated in figure 2 (Bush et al., 1999). In demye-

lination, it was reported that astrocytes recruit microglia to engulf myelin debris helping to promote remyelination. Hence, astrocytes play a dual role beneficial and damaging in the same time.

Microglia are the resident immune cells of the CNS. They play different roles from acting as antigen presenting cells (APCs), producing cytokines, to their involvement in phagocytosis. Activated microglia are documented in all MS patients and specially in progressive subtypes.

They produce cytotoxic and pro-inflammatory cytokines, reactive oxygen and nitrogen intermediates (Merson et al., 2010). Microglia are likely to be an important player in the MS damage process, and are particularly involved in axonal injury (Howell et al., 2010). On the other hand, microglia may play a promoting role by secreting brain derived neurotrophic factor (BDNF), neurotrophin-3 (NT3), insulin growth factor (IGF-1) (Gandhi et al., 2010).

Microglia activation is a complex two-way process represented by a gradual transformation of resting microglia into different activated phenotypes (Kettenmann et al., 2011).

As a result of this complex and multistage process it is almost impossible to define a distinct microglial status based on morphology or surface markers, shown in figure 4. The so-called activated microglia M1 (neurotoxic phenotype) and M2a-c (neuroprotective phenotypes), seems to be an oversimplification (Ransohoff et al., 2009; Chhor et al., 2013; Peterson et al., 2014).

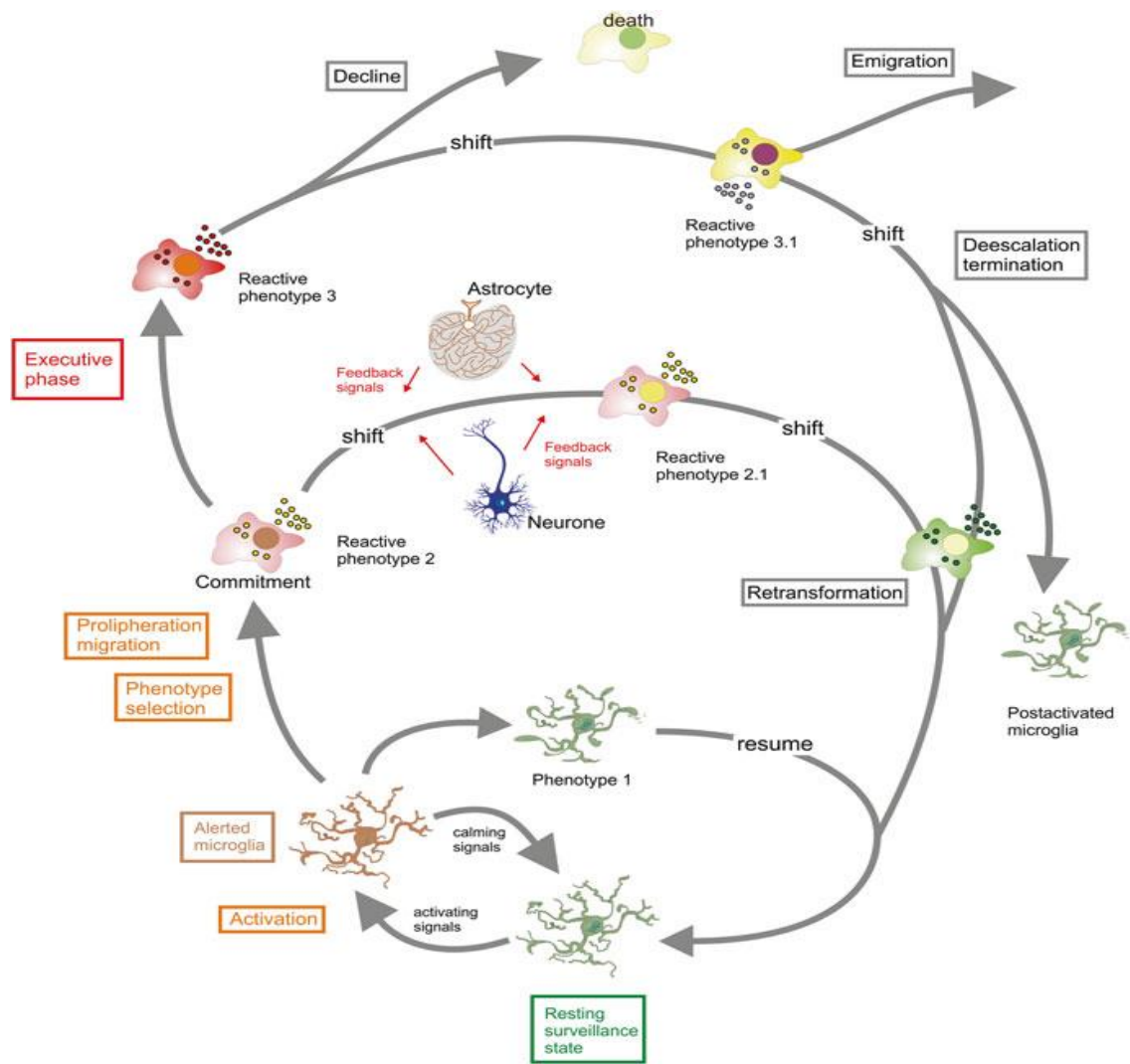


**Figure 3: Microglial activation as a continuous multistage process (Kettenmann et al., 2011).**

Oligodendrocytes loss and axonal damage leading to demyelination and astrocytic scars formation can be observed in variable degrees in MS throughout the CNS. They die by apoptosis before the formation of demyelinating plaques (Artemiadis et al., 2010). As reported, activated astrocytes and microglia secrete different cytotoxic cytokines and free radical species under stress and inflammation. Oligodendrocytes are sensitive to oxidative stress because of the high metabolic rate to synthesize myelin. Thus, it was proposed that intrinsic apoptosis caused by oxidative stress is a major cause for oligodendrocyte loss in MS.

Thus how these cells act in de- and remyelination and orchestrate together is a major path to understand MS better.

• Cell based
- CD4+ T cells sensitized to myelin antigens
- Antigen-specific cytotoxic CD8+ T cells
- Astrocyte disturbance
• Immune system factors
- Proinflammatory cytokines
- Demyelinating antibodies
- Complement cascade components
- Bystander demyelination following infectious super antigen cell activation
• Hypoxic/ischemic stress
- Reactive oxygen or nitrogen species
• CNS tissue infection
• Axonal dysregulation with secondary myelin loss
• Excitatory amino acids
- Glutamate
• Proteolytic, lipolytic enzymes
• Fas antigen–ligand interactions

**Table 1: Possible basis for myelin and oligodendrocyte injury in MS (Syed and Rizvi, 2011).**

During demyelination, astrocytes recruit microglia to engulf myelin debris; at this time oligodendrocyte precursor cells (OPCs) of adult CNS stem/precursor cells differentiate to mature oligodendrocytes to start remyelination. OPCs are the main source of remyelination; without these cells recovery and remyelination would be impossible. But remyelination in MS is ultimately limited and often fails. As suggested, one of the main reasons of this failure is that the reactive astrocytes partially suppress the adequate proliferation and differentiation of OPCs to form mature myelin-producing oligodendrocytes. The exact basis for

oligodendrocyte and myelin loss is still up to date not fully understood (Mi et al., 2009).

Demyelination is not always permanent in MS, thus spontaneous remyelination occurs after demyelination, but in most cases it is not complete especially in the chronic phases of the diseases where the OPCs reservoir is overwhelmed (Lucchinetti et al., 1999). FTY720, a sphingosine-1-phosphate receptor modulator used in the treatment of relapsing MS subtypes, was reported to enhance myelin repair in a kindling mouse model. Therefore, sphingolipids could be a major research focus in helping to achieve faster and complete remyelination (Gol et al., 2017).

### **1.8 Sphingolipids and Acid Sphingomyelinase**

Sphingolipids are structural and functional components of all biological membranes, consisting of over 100 bioactive lipids, involved in many cellular functions (Ogretmen and Hannun 2004; Ponnusamy et al., 2010; Chen et al., 2012; Podbielska et al., 2012).

Sphingolipids share a sphingosine (2-amino-4-octadecene-1, 3-diol) backbone linked via an amide bond to a fatty acid (forming ceramide), or being phosphorylated forming sphingosine- 1-phosphate. Ceramide can be modified to form glycosphingolipids, sphingomyelin, or ceramide-1-phosphate, see figure 5. The metabolism of sphingolipids is highly sophisticated and carefully regulated (Mullen et al., 2012). In the recent years, sphingolipids were increasingly linked and reported to play important roles in the pathophysiology of several neuroinflammatory diseases, especially MS, but also others such as stroke, dementia and inflammatory neuropathies (Gulbinn et al., 2013).

The exact function of spingolipids in neuroinflammation is not fully understood, it includes different mechanisms; apoptosis, astrogliosis, leukocyte activation, leukocyte trafficking and receptor clustering (Jana and Pahan, 2010; Gulbins et al., 2013, Maceyka et al., 2014). Nervous system cell subtypes have a vast repertoire of spingolipids. S1P receptors are widely expressed in brain cells (Yu et al., 2012; Choi and Chun 2013).

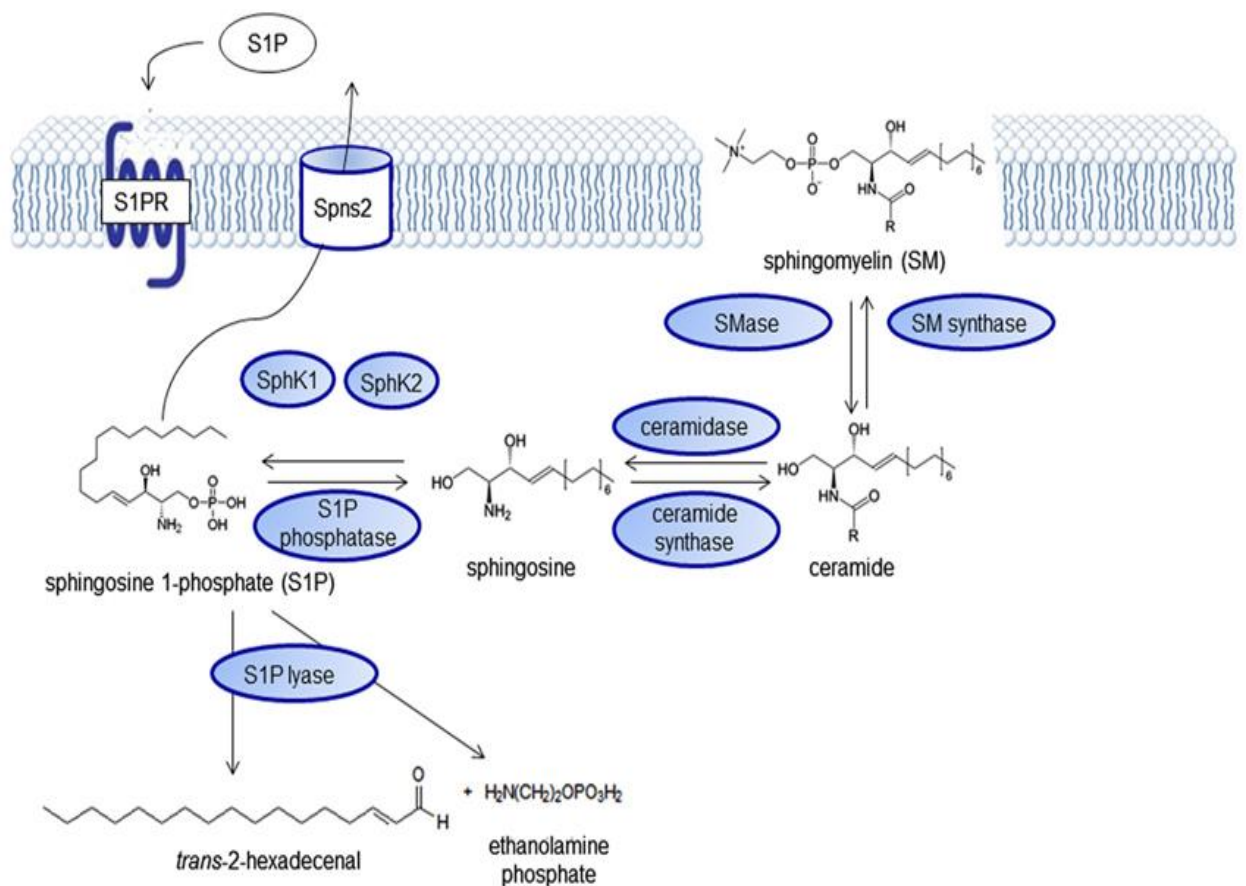


**Figure 5: The spingolipid signaling pathway (Brunkhorst et al., 2014).**

Studies reported the inhibition of sphingosine kinase or S1P receptor decreases astroglial proliferation as well as gliosis (Wu et al., 2008). As mentioned earlier, FTY720 - the S1P agonist - was applied to TNF $\alpha$ -treated human astrocytes, and showed a reduction in the release of monocyte chemotactic protein-1, docu-

menting decreased pro-inflammatory reaction of astrocytes (Van Doorn et al., 2010).

Sphingomyelinases are a family of enzymes that catalyze the breakdown of sphingomyelin into ceramide. Discovered in 1940 by Thannhauser and Reichel (Thannhauser, 1940), Acid sphingomyelinase (ASM) was first clearly described by Gatt (Gatt, 1963). The gene responsible for ASM is SMPD1, found on chromosome 11p15.4; encoding a 629 amino acid polypeptide (Schuchman et al., 1992). It has a lysosomal form (75 kDa) and a secreted form (57 kDa) (Ferlinz et al., 1994).

ASM converts sphingomyelin to ceramide releasing it in the outer layer of the cell membrane causing the formation of ceramide-rich microdomains fusing together. And forming rafts which re-organize cell signaling proteins, cluster receptor molecules and amplify signals (Bianco et al., 2009; Gulbins and Li, 2006; 2013). Also, the stimulation of T or B cells (via the co-stimulatory receptors, CD28 and CD40, respectively) led to the activation of acid sphingomyelinase (ASM) and release of ceramide (Stoffel et al., 1998; Gulbins et al., 2013).

ASM was shown to be activated by the inflammatory cytokines TNF $\alpha$  and IL-1, as well as by oxidative stress. As mentioned, ASM was reported to be upregulated in reactive astrocytes in MS lesions. Adding to this, ASM-derived ceramide decreases the barrier function of brain endothelial cells at the BBB (Kim Hye et al., 2011; Kim SunJa et al., 2012; Lopes. et al., 2016).

### **1.8.1 Sphingolipids in MS and de/remyelination**

Research concerning sphingolipids and its implication in MS has been significantly increased in the past years. But still more research is needed to under-

stand this complex interaction. Studies showed the presence of anti-sphingomyelin antibodies in the cerebrospinal fluid (CSF) of MS patients, in addition to that it was reported its role in apoptosis, T cell trafficking, astrocyte activation and receptor clustering (Kanter et al., 2006; Jana and Pahan, 2007; Wu et al., 2008; Yuan et al., 2012; Gulbins et al., 2013).

De- and remyelination are major research focus in MS. Thus, the sphingosine-1-phosphate analogue Fingolimod, a broadly used MS treatment, has been shown to enhance cell survival of human oligodendrocytes *in vivo* (Miron et al., 2008; Brunkhorst et al., 2014) and to reduce demyelination in cuprizone-treated mice by indirect effects on glial cells (Kim et al., 2011; Gol et al., 2017).

ASM hydrolyses sphingomyelin to ceramide which was linked to apoptotic signaling and the formation of ceramide-enriched platforms. Ceramide was also described to be increased in CSF of MS patients (Vidaurre et al., 2014). And exposure of rat neurons to ceramide containing CSF can lead to neuronal mitochondrial and axonal damage (Vidaurre et al., 2014). Again, astrocytes seem to play a detrimental role as they have been described as main cellular source for ceramide production in human MS brains with high levels of ASM mRNA (van Doorn et al., 2010). As potential therapeutic approach, ASM function can be inhibited by well-known drugs, such as tetracyclic anti-depressants, e.g. amitriptyline (Kim Hye et al., 2011; Kim SunJa et al., 2012; Kornhuber et al., 2010).

Studies documented that inhibitors of ASM such as fluoxetine attenuate the development of EAE in mice decreasing neuroinflammation (Yuan et al., 2012; Verderio et al., 2012). Similar phenotype was observed in *Smpd1*<sup>-/-</sup> rats that develop a milder clinical course of EAE together with decreased immune cell infiltration to the spinal cord (Yuan et al., 2012). These reports suggest that

there is a direct effect and a major role of Acid sphingomyelinase on T cell transmigration in EAE (Yuan et al., 2012; Verderio et al., .2012). In addition, recent evidence by Lopes et al.,2016 show the involvement of ASM and ceramide in the process of T cell migration via ICAM-1 (Intercellular Adhesion Molecule-1) function. It was reported that activated ASM and the formation of ceramide lipid rafts provide the proper conditions for ICAM-1 clustering.

In demyelination and neuroinflammation in general astrogliosis and microgliosis occur (Gudi et al., 2014). Also, ASM was reported to be upregulated in reactive astrocytes in MS lesions (Kim Hye et al., 2011). Also using FTY720, a S1P agonist, in the toxic demyelination model resulted in a decreased demyelination compared to untreated animals and increased oligodendrocyte survival *in vivo* (Kim Hye et al., 2011; Gol et al., 2017). Therefore, sphingolipids play an important part in the demyelination pathway. Hence, the inhibition of ASM by amitriptyline, an FDA approved selective serotonin release inhibitor (SSRIs), could have direct or indirect effect on de-or remyelination is to be evaluated.

## 2 Aim of work

We chose to study the acid sphingomyelinase/ceramide system in multiple sclerosis animal models, as it was reported earlier to play a role in apoptosis, receptor clustering and neuroinflammation. The ability to inhibit acid sphingomyelinase activity with available ready-to-use pharmacologic agents, such as amitriptyline, that have minimal side effects and have been in clinical use is a great advantage.

The aim of this work was to study and identify the role of acid sphingomyelinase in MS pathophysiology in two different MS animal models. The chronic experimental autoimmune encephalomyelitis model giving the opportunity to observe the infiltration of T cells to the CNS with the break-down of the blood-brain barrier. The cuprizone model, a toxic demyelination model, where the blood brain barrier remains intact, allows the study of de- and remyelination without the interference of the adaptive immune system.

We hypothesized that the inhibition of acid sphingomyelinase, either by genetic knockout or by pharmacological inhibition attenuates the outcome of chronic EAE. As a second approach, if our hypothesis proved correct, then acid sphingomyelinase deficiency affects T cell infiltration to the CNS in the chronic EAE model.

Using the cuprizone model we hypothesized that the inhibition of ASM either by genetic knockout or by pharmacological inhibition plays a role in de- and/or remyelination in the toxic demyelination model. And a positive outcome would be observed concerning the effect of ASM deficiency on axonal damage, astrogliosis, microgliosis and oligodendrocyte proliferation in experimental de- and remyelination.

## 3 Materials and methods

### 3.1 Materials

#### 3.1.1 Instruments

Instruments	Company
7500 Fast Real-Time PCR System	Applied Biosystems (Darmstadt, Germany)
Accu jet Pipettes Control	BrandTech Scientific (Essex, CT, USA)
Autoclave 3870 ELV	Systec (Wettenberg, Germany)
Autoclave V-150	Systec (Wettenberg, Germany)
Axiovert 25 inverted Microscope	Carl Zeiss Microscopy (Jena, Germany)
Axiovert 40 CFL Microscope	Carl Zeiss Microscopy (Jena, Germany)
Biofuge 13 Centrifuge	Heraeus (Hanau, Germany)
Biowizard KR-200 Bench	Kojair Tech Oy (Vilppula, Finland)
Eclipse TS100 Inverted Microscope	Nikon Instruments (Melville, NY, USA)
Eclipse E600 Fluorescence Microscopy	Nikon Instruments (Melville, NY, USA)
Epson perfection V700 photo scanner	Epson (Munich, Germany)
Freezer Premium no frost	Liebherr (Lindau, Germany)
Freezer UF75-110 T	Colora (Frankfurt, Germany)
Forced-air laboratory freezer	Liebherr (Ochsenhausen, Germany)
Forced-air laboratory refrigerator	Liebherr (Ochsenhausen, Germany)
General Rotator STR4	Stuart Scientific (Staffordshire, UK)
Ice Machine	Eurfrigor Ice Makers Srl (Lainate, Italy)
InoLab pH 720 pH-meter	WTW (Weilheim, Germany)
Laboratory balance ALS120-4, EW4200, EW420	Kern & Sohn (Balingen, Germany)
Laboratory centrifuge SIGMA 4K15C	Sigma Laborzentrifugen GmbH (Osterode am Harz, Germany)
Leica SM 2000 R Sliding Microtome	Leica Microsystems Nussloch GmbH (Nussloch, Germany)
Leica TP1020 Tissue Processor	Leica Microsystems Nussloch GmbH (Nussloch, Germany)
Leica EG1150C Cold plate	Leica Microsystems Nussloch GmbH (Nussloch, Germany)
Leica EG1150 H Heated Paraffin Embedding Module	Leica Microsystems Nussloch GmbH (Nussloch, Germany)
Liquid Nitrogen Container	KGW-Isotherm (Karlsruhe, Germany)
Micro-plate reader	TECAN, Sunrise Remote (Männedorf, Switzerland)
Microscope Zeiss Axio Scope	Carl Zeiss (Göttingen, Germany)
MLA-130 Rotor, Fixed Angle, Titanium for Ultra-centrifuge	Beckman Coulter (Brea, USA)
Multiband UV table	Peqlab (Karlsruhe, Germany)
Multipette® plus	Eppendorf (Hamburg, Germany)
Nanodrop ND-1000 Spectrophotometer	PEQLAB Biotechnologie (Erlangen, Germany)
Pipette PIPETMAN	Gilson (Middleton, WI, USA)
Pipette Single-Channel	Eppendorf (Hamburg, Germany)
Pipette Pipetus	Hirschmann (Eberstadt, Germany)
Precision Balance scale 770	Kern & Sohn (Balingen, Germany)
Precision Balance scale CP 42023	Sartorius (Göttingen, Germany)
PTC 200 DNA Engine Thermal Cycler	MJ Research (St. Bruno, Canada)

PURELAB Ultra Water Purification system	Elga (Celle, Germany)
Refrigerator KG39VVI30	Siemens (München, Germany)
Rocky 3D	Labortechnik Frübel (Lindau, Germany)
Savant SpeedVac DNA 110	Thermo Scientific (Langenselbold, Germany)
Shakers SM-30	Edmund Bühler (Hechingen, Germany)
Tabletop Centrifuge 4K10	Sigma Laborzentrifugen (Osterode am Harz, Germany)
Tabletop Centrifuge 4K15C	Sigma Laborzentrifugen (Osterode am Harz, Germany)
Thermoblock TDB-120	BioSan (Riga, Latvia)
Thermomixer comfort	Eppendorf (Hamburg, Germany)
Vortex Genie 2	Scientific Industries (Bohemia, NY, USA)
Vortex Shaker REAX 2000	Heidolph (Schwabach, Germany)
Water bath	Köttermann (Hänigsen, Germany)

### 3.1.2 Experimental material

Experimental materials	Company
Beakers	VWR (Darmstadt, Germany)
Biosphere Filter Tips (10 µl, 200 µl, 1000 µl)	Sarstedt (Nümbrecht, Germany)
BD Plastipak syringe, 1ml	Becton, Dickinson and Company (Heidelberg, Germany)
Bottle Top Filter 500ml, 0.22mm	Sarstedt (Nümbrecht, Germany)
Centrifugentubes (15 ml, 50 ml)	Sarstedt (Nümbrecht, Germany)
Combitips Plus (5 ml, 10 ml)	Eppendorf (Hamburg, Germany)
CryoPure tubes 1.8 ml	Sarstedt (Nümbrecht, Germany)
Cuvettes	Sarstedt (Nümbrecht, Germany)
Dako pen	Dako (Glostrup, Denmark)
Erlenmeyer Flasks	Schott (Mainz, Germany)
Falcon Round bottom test tubes 5 ml	BD Biosciences (Heidelberg, Germany)
Glass Bottles	Fisher Scientific (Schwerte, Germany)
Gloves, Nitril	VWR (Darmstadt, Germany)
Hemocytometer	Brand (Wertheim, Germany)
Homogenizer	Hartenstein, (Würzburg, Germany)
Isoflurane	Baxter (Unterschleißheim, Germany)
Laboratory glassware	Schott (Mainz, Germany)
Luerlock syringe 1 ml	BD Biosciences (Durham, USA)
Microscope slides 76 ´ 26 mm	Gerhard Menzel (Braunschweig, Germany)
15 ml, 50 ml, round bottom 50 ml conical centrifuge tubes	Sarstedt (Nümbrecht, Germany)
Parafilm M all-purpose laboratory film	Pechiney Plastic Packaging (Chicago, USA)
pH-indicator Strips pH 0 - 14 universal indicator	Merck (Darmstadt, Germany)
Pipette tip 10 µl, 200 µl, 1000 µl	Sarstedt (Nümbrecht, Germany)
Syringe filter 0.22 µm	Carl Roth (Karlsruhe, Germany)
Syringe, 2ml, 5ml, 10ml, 20ml	B Braun (Tuttlingen, Germany)

## 3.1.3 Chemicals

Chemicals	Company
(3-Aminopropyl) triethoxysilane	Sigma Aldrich (Taufkirchen, Germany)
2-methyl butane	Sigma Aldrich (Taufkirchen, Germany)
2-Propanol	Carl Roth (Karlsruhe, Germany)
Agarose	Biozym (Oldendorf, Germany)
Acetone	Hedinger (Stuttgart, Germany)
Amino-ethylcarbazol (AEC)	Sigma-Aldrich Chemie (Steinheim, Germany)
Amitriptyline	Sigma (Schnelldorf, Germany)
Ammonium chloride	Sigma-Aldrich Chemie (Steinheim, Germany)
Antibiotic-antimycotic	Invitrogen (Darmstadt, Germany)
Aquatex	Merck (Darmstadt, Germany)
Bovine Serum Albumin (BSA)	Sigma Aldrich (Taufkirchen, Germany)
Casein	Fluka (Buchs, Switzerland)
Citrate acid	Serva (Heidelberg, Germany)
Cuprizone	Sigma Aldrich (Taufkirchen, Germany)
Dimethyl sulfoxide (DMSO)	Sigma Aldrich (Taufkirchen, Germany)
Diaminobenzidin-Hydrochlorid (DAB)	Sigma Aldrich (Taufkirchen, Germany)
DNA Ladder (100 bp, 1 kb)	New England Biolabs (Frankfurt am Main, Germany)
dNTP Mix	Roche (Mannheim, Germany)
Dithiothreitol (DTT)	Sigma Aldrich (Taufkirchen, Germany)
Entellan@mouting media	VWR (Darmstadt, Germany)
Ethidiumbromid	Carl Roth (Karlsruhe, Germany)
Ethanol	Sigma Aldrich (Taufkirchen, Germany)
Glycerol	Sigma Aldrich (Taufkirchen, Germany)
H <sub>2</sub> O <sub>2</sub>	Otto Fishar (Saarbrueken, Germany)
HCl	Sigma Aldrich (Taufkirchen, Germany)
Hexamer Random Primer	Invitrogen (Darmstadt, Germany)
Isoflurane	Baxter (Unterschleißheim, Germany)
Incomplete Freund Adjuvant	DIFCO Laboratories (Michigan, USA)
Isopropanol	Carl Roth (Karlsruhe, Germany)
Lithium Carbonate	Sigma Aldrich (Taufkirchen, Germany)
Luxol Fast Blue (LFB)	RAL diagnostics (Martillac, France)
KHCO <sub>3</sub>	Merck (Darmstadt, Germany)
KCl	Merck (Darmstadt, Germany)
MgCl <sub>2</sub>	Fluka (Buchs, Switzerland)
Mayers Hematoxylin	VWR (Darmstadt, Germany)
Methanol	Sigma Aldrich (Taufkirchen, Germany)
Mycobacterium tuberculosis H37 Ra	BD Biosciences (Durham, USA)
Myelin Oligodendrocytic peptide <sup>35-55</sup>	Charite (Berlin, Germany)
Paraformaldehyd (PFA)	Merck (Darmstadt, Germany)
Pertussis toxin	Enzo life Sciences (Lörrach, Germany)
Periodic Acid	Merck (Darmstadt, Germany)
Schiff's reagent	Merck (Darmstadt, Germany)
Sodium acetate	Merck (Darmstadt, Germany)
Sucrose	VWR (Darmstadt, Germany)

Sodium carbonate	Sigma-Aldrich Chemie (Steinheim, Germany)
Triton X-100	Sigma Aldrich (Taufkirchen, Germany)
TRizol	Sigma Aldrich (Taufkirchen, Germany)
Tween 20	Sigma Aldrich (Taufkirchen, Germany)
Tissue Tek	Sakura Finetech Europe (Amsterdam, Netherlands)
Trypan Blue	Sigma-Aldrich Chemie, Steinheim, Germany)
Xylene	Otto Fischar (Saarbrücken, Germany)

### 3.1.4 Kits

Kit	Company
Vectastain Elite ABC kit Rat IgG	Vectastain (Wertheim-Bettingen, Germany)
DyNAmo™ Flash SYBR Green qPCR Kit	Roche Applied Sciences (Mannheim, Germany)
SuperScript® III Reverse Transcriptase	Invitrogen (Darmstadt, Germany)

### 3.1.5 Oligonucleotides

Gene	Primer forward 5' - 3'	Primer reverse 5' - 3'
<i>mouse GAPDH</i>	ACAAC TTTGGCATTGTGGAA	GATGCACGGATGATGTTCTG
<i>mouse Il-1<math>\beta</math></i>	GAAGAAGAGCCCATCCTCTG	TCATCTCGGAGCCTGTAGTG
<i>mouse FGF1</i>	TTTATACGGCTCGCAGACAC	GCTTACAGCTCCCGTTCTTC
<i>mouse Mrc1</i>	TGATTACGAGCAGTGGAAGC	GTTCCACCGTAAGCCCAATTT
<i>mouse FGF2</i>	CCAACCGGTACCTTGCTATG	TATGGCCTTCTGTCCAGGTC

### 3.1.6 Antibodies

Antibody	Company
<i>mouse monoclonal anti Iba-1 Clone, 20A12.1</i>	Millipore (Schwalbach, Germany)
<i>rabbit polyclonal anti Iba-1</i>	Wako (Neuss, Germany)
<i>rabbit polyclonal anti CD3 (ab5690)</i>	Abcam (Cambridge, UK)
<i>mouse monoclonal anti Synaptophysin (ab8049)</i>	Abcam (Cambridge, UK)
<i>rabbit polyclonal anti Olig-2 ab81093</i>	Abcam (Cambridge, UK)
<i>rabbit polyclonal anti MBP (ab40390)</i>	Abcam (Cambridge, UK)
<i>Biotin SP conjugated goat anti mouse (ab128976)</i>	Abcam (Cambridge, UK)
<i>rabbit polyclonal anti APP (a8717)</i>	Sigma-Aldrich (St. Louis, USA)
<i>rat monoclonal anti GFAP (13-0300)</i>	Invitrogen (Darmstadt, Germany)
<i>goat anti rabbit Alexa 488 Conjugate (1670152)</i>	Invitrogen (Rockford, USA)
<i>Biotin SP conjugated Affinipure goat anti rabbit IgG(H+L)</i>	Jackson Immunoresearch Laboratories (Baltimore, USA)

**3.1.7 Buffers and media**

Recipe	Chemicals	Amount	Concentration
10X Citric buffer	Citric acid	2.014g Up to 1 Liter	10mM
10x PBS	NaCl KCl Na <sub>2</sub> HPO <sub>4</sub> NaH <sub>2</sub> PO <sub>4</sub> x H <sub>2</sub> O dest. H <sub>2</sub> O Adjust to pH 7.4	400g 10g 71g 69g Up to 5 liters	1.37 M 27 mM 100 mM 100 mM
10x TBS	Tris NaCl dest. H <sub>2</sub> O Adjust to pH 7.4	302.5 g 425 g Up to 5 Liter	500 mM 1.45 M
5x TBE	Tris Borat 0.5 M EDTA [pH 8.0] dest. H <sub>2</sub> O	270 g 137.5 g 100 ml Up to 5 Liter	446 mM 446 mM 10 mM
Blocking buffer	PBS Casein Tween 20 Triton X		As needed 0.02% 0.1 % 0.01%
4% PFA	dest. H <sub>2</sub> O NaOH PFA 10X PBS	Up to 1 liter 100µl 40g 100 µl	10N

**3.2 Methods**

**3.2.1 Mice**

Acid sphingomyelinase genetically deficient mice (*Smpd1*<sup>-/-</sup>; protein: ASM, gene symbol: *Smpd1*) and wild type (C57BL/6J) littermates were obtained from our breeding facility (Forschungs- und Verfügungsgebäude der Medizinischen Fakultät des Universität des Saarlandes, 61.4). All mice were maintained in a pathogen-free environment. Food and water were available *ad libitum*. The genotype of the *Smpd1*<sup>-/-</sup> mice was confirmed by polymerase chain reaction (PCR) prior to experimentation. All animal experiments were approved by the regional council in Saarland, Germany.

Experiments were ended when animals lost more than 15% of weight. To that concern twelve animals dropped out from the chEAE experiments. Paralyzed animals were given HydroGel and food pellets placed at the base of the cages. All animal experiments were performed in the experimental surgery laboratory (Medizinischen Fakultät des Universität des Saarlandes, 65) and neuroimmunology laboratory (Medizinischen Fakultät des Universität des Saarlandes, 90).

### **3.2.2 Immunization, clinical scoring guide and treatment protocols**

#### **3.2.2.1 MOG emulsion preparation**

The emulsion used for immunization was prepared by combining MOG<sub>aa35-55</sub> with 10 mg/ml CFA in a 1:1 ratio in a latex-free syringe, for an end concentration of 300 µg MOG/200 µl. The solution was mixed manually with a pipette for 1 min and put on ice. The solution was then homogenized using a probe sonicator for 60 sec (2 cycles, 45% power) and again put on ice for 1 min.

The sonication was repeated as previous and then the reagent frozen at -20°C for 24 h. After 24 h, the emulsion was thawed and the 2 cycles of sonication (as described above) were repeated. The emulsion was either injected immediately or stored at -20°C for up to one week.

#### **3.2.2.2 Immunization**

Induction of chronic EAE (chEAE) in 6-8 weeks old (*Smpd1*<sup>-/-</sup> and wildtype) female mice was achieved by injecting 200 µl of the MOG emulsion, as prepared above, subcutaneously into the axillary and inguinal lymph node regions (50 µl/lymph node region) at day 0 and day 7. On days 0 and 2, 300 ng pertussis toxin dissolved in PBS up to a volume of 200 µl was injected intra-peritoneally (i.p.).

### 3.2.2.3 Clinical scoring guide

Clinical disease was checked daily and scored as previously described (Engelhardt et al., 1997):

- 0.5: Limp tail
- 1: Hind leg weakness
- 2: Hind leg paraparesis.
- 3: Hind leg paraplegia and incontinence
- 4: Fore limb and hind leg paresis.
- 5: Death

### 3.2.2.4 Amitriptyline treatment protocol

At the start of weight loss between days 12 and 16 post-immunization (Fig.I) and continuing for 8 days, 25 mg/kg amitriptyline dissolved in sterile distilled water was injected i.p. every 12 h in WT chEAE mice. The bi-daily (b.i.d.) dosing schedule was chosen to maintain a constant plasma level of amitriptyline (Teichgraber et al., 2008). Sterile PBS was injected as control.

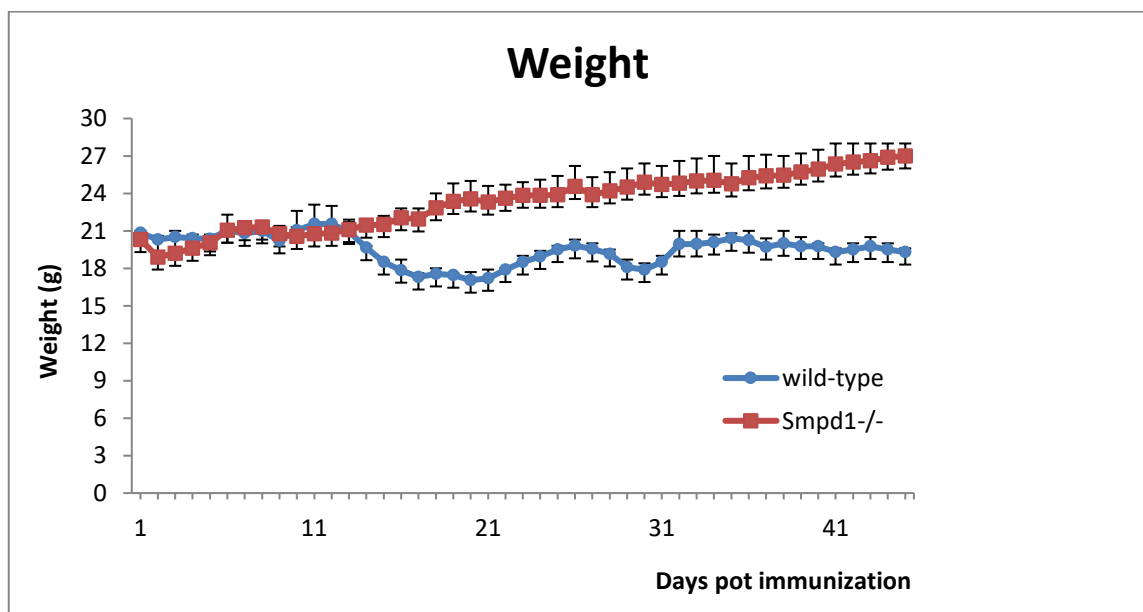


**Figure 4: Weight measurements of Smpd1 genetically deficient mice and wild-type littermates during chEAE.**

### **3.2.3 Induction of experimental de- and remyelination, treatment groups and amitriptyline treatment**

#### **3.2.3.1 Cuprizone diet**

Induction of demyelination was achieved by feeding 8 weeks old (Smpd1<sup>-/-</sup> and wildtype) male littermate mice with 0.2% cuprizone mixed freshly everyday into grounded standard rodent chow. The cuprizone diet was maintained for 5 weeks (acute demyelination) or 12 weeks (chronic demyelination) see below; different experimental groups. To study remyelination, the cuprizone diet was replaced with normal diet for 1 or 2 weeks to allow recovery.

#### **3.2.3.2 Different experimental groups**

5 weeks acute demyelination (n=mice number)

- C57BL/6J + normal chow (control) (n=5)
- Smpd1<sup>-/-</sup> + normal chow (control) (n=5)
- C57BL/6J + cuprizone (n=5)
- Smpd1<sup>-/-</sup> + cuprizone (n=5)
- C57BL/6J + normal chow with 1 week Amitriptyline treatment (baseline) (n=5)
- C57BL/6J + cuprizone with 1 week PBS injections (control) (n=5)
- C57BL/6J + cuprizone with 1 week Amitriptyline treatment (n=5)
- C57BL/6J + cuprizone with 2 weeks Amitriptyline treatment (n=5)

Remyelination after 5 weeks demyelination

- C57BL/6J + cuprizone and 1 week recovery (n=5)
- Smpd1<sup>-/-</sup> + cuprizone and 1 week recovery (n=5)
- C57BL/6J + cuprizone and 1 week recovery + Amitriptyline treatment (n=5)
- C57BL/6J + cuprizone and 2 weeks recovery (n=5)
- C57BL/6J + cuprizone and 2 weeks recovery + Amitriptyline treatment (n=5)
- C57BL/6J + cuprizone and 2 weeks recovery + PBS (n=5)
- Smpd1<sup>-/-</sup> + cuprizone and 2 weeks recovery (n=5)

12 weeks chronic demyelination

- C57BL/6J + 12 weeks cuprizone (n=5)
- Smpd1<sup>-/-</sup> + 12 weeks cuprizone (n=5)

Remyelination after 12 weeks demyelination

- C57BL/6J + 12 weeks cuprizone and 2 weeks recovery (n=5)
- Smpd1<sup>-/-</sup> + 12 weeks cuprizone and 2 weeks recovery (n=5)

### 3.2.3.3 Amitriptyline treatment protocol

For all of the amitriptyline treated groups, 25 mg/kg amitriptyline dissolved in sterile distilled water was injected i.p. every 12 h, as mentioned previously, for a treatment period of 2 weeks. Sterile PBS was used as control.

## 3.3 Tissue collection

For the chEAE groups, mice were scarified at day 45 p.i. and perfused via the left cardiac ventricle with ice-cold PBS followed by 4% PFA in phosphate buffer. Brains and spinal cords were harvested, and either dehydrated for paraffin embedding or placed in Tissue-Tek and snap-frozen in isopentane with liquid nitrogen at -80°C for cryo-sectioning. The frozen tissue was cut in 25µm or 10 µm sections on a cryostat and fixed with acetone at -20°C. Paraffin embedded spinal cords were also sectioned in 25µm sections on a microtome. Both frozen and paraffin-embedded tissue sections were placed on silanized slides to ensure adherence during staining protocols. For the de-remyelination groups, mice were anesthetized with isoflurane and perfused via the left cardiac ventricle with PBS for gene expression analysis or with 4% PFA for immunohistochemistry studies. Brains were collected post-fixed in 4% PFA and dehydrated for paraffin embedding. Tissues were coronally sectioned each 5µm in thickness on a microtome and dried at 37°C overnight. Sections between bregma -

0.82mm and bregma -1.82mm according to the mouse atlas by Paxinos and Franklin (2001) were analyzed. Before perfusion blood from amitriptyline treated animals was collected from the vena cava for later measurements of nortriptyline (data not shown).

## **3.4 Histology**

### **3.4.1 Luxol Fast Blue Stain (LFB)**

Demyelination in the corpus callosum was examined by staining coronal brain sections with Luxal fast Blue, staining myelin in blue and periodic acid-Schiff, staining demyelinated axons in pink. Detailed Procedure as follows:

1. Put LFB solution in 60°C oven.
2. De-paraffin slides in xylene (1) for 2 mins
3. De-paraffin slides in xylene (2) for 2 mins
4. Clear slides in 100% alcohol (1) for 2 mins
5. Clear slides in 100% alcohol (2) for 2 mins
6. Hydrate slides in 95% alcohol for 2 mins
7. LFB solution for 2 hours at 60°C
8. Take out let stand (cool) for 5 mins
9. Rinse in 95% alcohol to remove excess stain
10. Rinse in dest H<sub>2</sub>O for 2 mins
11. Differentiate in 0.05% lithium carbonate 4-5 dips
12. Differentiate in 70% alcohol until grey
13. Wash in H<sub>2</sub>O for 1 min
14. 0.5% periodic acid for 5 mins
15. Schiff's reagent for 15 mins
16. Wash in running tap water for 10 mins
17. Hematoxylin for 20-40 seconds
18. Wash in running tap water for 2 mins
19. Dehydrate in 95% alcohol for 30 seconds
20. Dehydrate in 100% alcohol (3) for 1 min
21. Dehydrate in 100% alcohol (4) for 2 mins

22. Clear in Xylol (3) for 2 mins
23. Clear in Xylol (4) for 2 mins
24. Mount in Entellan

### 3.5 Immunohistochemistry

#### 3.5.1 GFAP, Iba-1, CD3, Olig-2, synaptophysin and APP staining

In order to quantify astrogliosis, microgliosis, oligodendrocyte cell numbers and axonal damage for the de- and remyelination groups. 5µm coronal sections from the brains of treated animals were cut and mounted on silanized slides and stained for primary antibodies. For the chEAE animals 25µm serially sectioned spinal cords were used to quantify CD3 positive cell numbers, astrogliosis and microgliosis in Smpd1 genetically deficient mice and corresponding WT littermates. The immunohistochemical staining was performed as follows on paraffin sections:

1. The slides were serially deparaffinized in the solutions (2 x 5 min Xylene, 2 x 5 min 100% ethanol, 5 min 96% ethanol, 5 min 70% ethanol, and 5 min 50% ethanol).
2. Antigen retrieval by cooking the sections in 1x citrate buffer (10 mM, pH 6.0) in a Microwave oven, 560 watts, 3 min x 5 times. Refill with buffer between each cooking. Cool down slowly by leaving on the bench for >30 min after cook.
3. The endogenous peroxidase of the tissue was inactivated via incubating the slides in the mixture of H<sub>2</sub>O<sub>2</sub> /Methanol/dH<sub>2</sub>O buffer, RT, 30min.
4. Wash slides with TBS, 5 min x 2 times and then with TBS-T, 5 min, once.
5. Block with blocking buffer (0.2% Casein (w/v) + 0.1% Tween 20 + 0.1% Triton X- 100 in PBS), RT, 1hr.
6. 1st Antibody reaction: Concentrations shown below. Diluted in dilution buffer (0.02% Casein (w/v) + 0.01% Tween 20 + 0.01% Triton X-100 in PBS), 100 µl/section, incubate at 4 °C, overnight.

7. Wash as step 4.
8. 2nd Antibody reaction: biotinylated goat-anti-rabbit or biotinylated goat-anti-mouse depending on the primary antibody. Concentrations shown below. Secondary antibody diluted in dilution buffer (0.02% Casein (w/v) + 0.01% Tween 20 + 0.01% Triton X-100 in PBS). Incubate at RT 1hr.
9. Meanwhile prepare avidin-biotin-enzyme-complex, ABC kit (Vectastain). Dilute reagent A and reagent B in PBS/T (both 1:100), 100 µl/section. Incubate in dark, at least 30min before use, allowing the formation of avidin-biotin HRP complex.
10. Wash as step 4.
11. Incubate with ABC reagent. RT, 1hr.
12. Wash as step 4.
13. Develop with DAB, 45 sec, and then wash with dH<sub>2</sub>O, 3 times
14. Counterstaining with Hematoxylin, 20 sec, forward to dH<sub>2</sub>O wash 3 times. Then develop in running tap water for 5 min, and then change back to dH<sub>2</sub>O.
15. Dehydration: serially treat the slides in the following solutions: water, 3 min, 50% ethanol, 3 min 70% ethanol, 3 min 96% ethanol, 2 x 3 min 100% ethanol, 2 x 5 min Xylene.
16. Mount the slides with Entellan (Merck), and then cover the tissue with cover glass.

Primary Antibody	Concentration	Company
Glial fibrillary acidic protein ( <b>GFAP</b> )	1:1000	<i>Invitrogen (Darmstadt, Germany)</i>
Ionized calcium-binding adapter molecule 1 ( <b>Iba-1</b> )	1:200	<i>Millipore (Schwalbach, Germany)</i>
Oligodendrocyte transcription factor ( <b>OLIG-2</b> )	1:1500	<i>Abcam (Cambridge, UK)</i>
Synaptophysin	1:50	<i>Abcam (Cambridge, UK)</i>
Amyloid precursor protein ( <b>APP</b> )	1:1000	<i>Sigma-Aldrich (St. Louis, USA)</i>
Cluster of differentiation-3 ( <b>CD3</b> )	1:100	<i>Abcam (Cambridge, UK)</i>
Secondary Antibody	Concentration	Company
Biotin conjugated Affinipure goat anti rabbit IgG(H+L)	1:200	Jackson Immunoresearch Laboratories (Baltimore, USA)
Biotin SP conjugated goat anti mouse (ab128976)	1 drop	<i>Abcam (Cambridge, UK)</i>

**Table 2: The used primary and secondary antibodies. Respective concentrations are summarized.**

### 3.5.2 MBP fluorescence staining

Brain coronal paraffin sections of 5µm thickness from mice of de-remyelination studies, stained with primary antibody against MBP to measure the fluorescence intensity of myelin in the corpus callosum were stained as follows:

1. The slides were serially deparaffinized in the solutions (2 x 5 min Xylene, 2 x 5 min 100% ethanol, 5 min 96% ethanol, 5 min 70% ethanol, and 5 min 50% ethanol).
2. Wash in PBS 5 mins.
3. Antigen retrieval by cooking the sections in 1× citrate buffer (10 mM, pH 6.0) in a Microwave oven, 560 watts, 3 min × 5 times. Refill with buffer between each cooking. Cool down slowly by leaving on the bench for >30 min after cook.
4. Wash in PBS-T, 5mins.
5. Block for 1hr (5% goat serum in PBS-T).
6. Primary antibody, rabbit polyclonal anti-MBP at 1:100 diluted in 1% goat serum in PBS-T.
7. Incubate overnight at 4°C.
8. Wash in PBS-T, 5 mins.
9. Add secondary antibody, *Alexa fluor 488* goat anti rabbit at 1:100 diluted in 1 % goat serum in PBS-T, 1hr at RT.
10. Wash in PBS, 5 mins.
11. Check for Fluorescence under microscope.
12. Mount with Mowiol.

### 3.6 Quantification of de- and remyelination

The midline corpus callosum as diagrammed below in Fig. 7 was examined (Mason et al., 2000). Sections between bregma -0.82 mm and bregma -1.82 mm according to the mouse atlas by Paxinos and Franklin (2001) were analyzed. All manual scorings were performed completely blind to the animal's genotype and the treatment group. The LFB stained sections were scored

based on the relative ratio of blue or pink fibers detected, on a scale from zero to three, three being completely myelinated and zero being completely demyelinated (Skripuletz et al., 2012). Five animals per group were included. Two to three slices (5 $\mu$ m) per animal was stained, taking two pictures per slide to be scored.

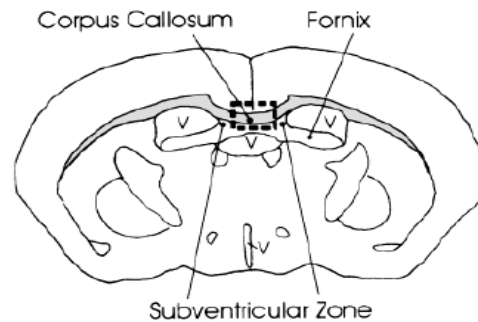


**Figure 5: Representation of the corpus callosum. And the level at which brain tissue sections were stained and scored in the CC for de- and re- myelination (v = ventricle) (Mason et al., 2000).**

### 3.7 Quantification of inflammation and lesions in spinal cords of chEAE mice

Longitudinally sectioned 5 $\mu$ m thick paraffin embedded spinal cords from chEAE experiments were stained with LFB/PAS. In the control tissue there is no influx of leukocytes or accumulation within the tissue. During chEAE there is evident infiltration of leukocytes observed in the pial lining and subsequently in the parenchyma. The number of lesions within a spinal cord section is also indicative of the degree of inflammation. Thus, by location and number (< or > 5) of lesions on each section, a qualitative score can be documented in blinded analyses, with ascending scores representing greater severity. Areas of inflammation (hypercellularity) are usually correspondent with area of demyelination where there is less LFB stain observed. For semiquantitative assessment of the

extent of inflammation in the spinal cord, all stained longitudinal sections were first evaluated using the scoring system outlined below (DaSilve et al., 2009).

Two to three different sections per animal were examined blindly without knowing the animal's genotype or the treatment group and the average number of lesions per section was documented (DaSilve et al., 2009).

**Table 3: Scoring system used for semi-quantitative assessment of the extent of inflammation.**

Score	Description
0	Normal
1	Pial inflammation only, <5 lesions/section
2	Pial inflammation only, >5 lesions/section
3	Beginning of parenchymal inflammation (moving into parenchyma from pia)
4	Parenchymal inflammation, <5 lesions/section
5	Parenchymal inflammation, >5 lesions/section (relatively small parenchymal lesions)
6	Parenchymal inflammation, >5 lesions/section (relatively large parenchymal lesions)
7	Parenchymal inflammation, with large lesions and holes in tissue

### 3.8 Quantification of oligodendrocyte and T-cell numbers

Quantification of oligodendrocytes in the cuprizone experiments was achieved by manual counting the number of Olig-2 positive cells in the investigated region. At least two sections per animal. Cell counting was performed using an Axiomager Z2 microscope (Zeiss, Germany) and a 20 or 40x objective in the medial Corpus Callosum (CCm). For the chEAE tissues 2-3 sections 25µm thick slides minimum 100µm apart were counted for CD3-positive cells in an area not less than  $11 \times 10^6 \mu\text{m}^2$  in the thoracic and lumbar regions of the spinal cord. Images were acquired using an Axiomager Z2 microscope equipped with a Stereo Investigator system (MicroBrightField). Cell numbers were calculated and expressed per  $\text{mm}^2$  for all histological analyses.

### 3.9 Quantification of astrocyte and microglia parameters

For astrocyte and microglia cell count in the cuprizone experiments, 2 to 3 sections (5µm) per animal were manually counted for GFAP and Iba-1 positive cells with clearly visible nucleus at the CCm. As an additional parameter for astrogliosis and microgliosis, the surface area covered by GFAP and Iba-1 staining was determined using a densitometric scanning procedure (ImageJ, Maryland, USA). Results are expressed as relative GFAP or Iba-1 covered area of the CCm (percentage of the stained area in relation to the non-stained area) (Zendedel et al., 2016). For the chEAE samples, at least 2 longitudinally sectioned spinal cord sections 25 µm in thickness with a distance of 150 µm in between were counted in an area not less than  $11 \times 10^6 \mu\text{m}^2$  in the thoracic and lumbar regions. All counting was done using an AxioImager Z2 microscope with an objective of 20x or 40x. Cell numbers are expressed as cells per  $\text{mm}^2$ . All morphological quantification was performed in a blinded way.

### 3.10 MBP fluorescence quantification

Quantification of MBP fluorescence intensity in the CCm of cuprizone treated mice was done using the ImageJ software. With the following formula:

*Fluorescence intensity = Integrated Density – (Area of the ROI x Mean fluorescence of background readings).*

Measurements were expressed as arbitrary units.

### **3.11 Reverse transcription and quantitative PCR for analysis of gene transcripts**

Real-time PCR is a quantitative method used to detect the number of PCR templates such as DNA or complementary DNA in a PCR reaction. Two types of real-time PCR are being used: intercalator-based and probe-based. Both protocols need a unique thermocycler set with a sensitive camera that measures the fluorescence in every well of the 96-well plate through the reaction. Intercalator-dependent method known as SYBR green procedure requires a double-stranded DNA dye in the PCR reaction which will bind to the newly synthesized double-stranded DNA, hence giving fluorescence. On the other hand, probe-dependent real-time PCR known as TaqMan needs a pair of PCR primers and an additional fluorescent probe - an oligonucleotide of 20-26 nucleotides with both a reporter fluorescent dye and a quencher dye attached. This probe is designed to bind only the DNA sequence between the two specific PCR primers. Solely a specific PCR product can generate a fluorescent signal in TaqMan PCR. In our study, real-time PCR was performed using SYBR green (Roche Applied Science) with the 7500 Fast Real-Time PCR System (Life Technologies).

#### **3.11.1 Corpus callosum RNA isolation with Trizol**

Following our laboratory protocol, corpus callosum was isolated from the whole brains under a light microscope. Then the total RNA was extracted from the tissue using Trizol (Life Technologies). First strand cDNA was synthesized by priming total RNA in addition to hexamer random primers (Life Technologies) with a Superscript III reverse transcriptase (Life Technologies). For quantifica-

tion of gene transcripts, real-time PCR was performed using SYBR green (Roche Applied Science) with the 7500 Fast Real-Time PCR System (Life Technologies). The quantity of the double-stranded PCR product produced was then measured by detecting the FAM dye freed from the SYBR green, which attaches to the double-stranded DNA. Threshold cycle (Ct) values for every test gene from the replicate PCRs were then normalized to the Ct values for *gapdh* control from the same cDNA prepared. Transcription ratios were calculated as  $2^{(\Delta Ct)}$  where  $\Delta Ct$  is the difference between Ct (*gapdh*) and Ct (test gene) (Liu Y. et al., 2014).

In detail:

1. Phase separation: Incubate the homogenized samples for 5 min at room temperature to permit complete dissociation of nucleoprotein complexes. Then add 0.2 ml of chloroform and shake vigorously by hand for 15 sec, and then incubate at room temperature for 3 min. Centrifuge the samples at 12,000 x g for 15 min at 4 °C. The sample mixture was separated into a lower red, phenol- chloroform phase, an interphase and a colorless upper aqueous phase. RNA remains in the aqueous phase.
2. RNA precipitation: Transfer the colorless aqueous phase to a fresh tube; precipitate the RNA from the aqueous phase by mixing with 0.5 ml isopropyl alcohol. Incubate at room temperature for 10 min and then centrifuge at 12,000 x g for 10 min at 4 °C. The precipitated RNA is the gel-like pellet on the bottom side of the tube.
3. RNA wash: remove the supernatant and wash the RNA once with 1 ml 75% ethanol. Mix by vortexing and centrifuge at 7,600 x g for 5 min at 4 °C.
4. Redissolve the RNA: briefly dry the RNA pellet, incubating for 10 min at RT and then dissolve it in appropriate volume of RNase-free water.

**3.11.2 Genome DNA degradation prior to RT-PCR**

To erase trace genomic DNA contamination in the RNA sample, RQ1 (RNA Qualified) RNase-Free DNase (Promega), which is a DNase-I that degrades both double-stranded and single-stranded DNA, was used.

This reaction was set up:

RNA sample in water	8 $\mu$ l
RQ1 RNase-Free DNase 10x Reaction buffer	1 $\mu$ l
RQ1 RNase-Free DNase	1 U/ $\mu$ g RNA
Nuclease-free water	To a final volume of 10 $\mu$ l

Incubate at 37 °C for 30 min, and then add 1  $\mu$ l of RQ1-DNase. Stop solution to terminate the reaction. The DNase was then inactivated by incubating at 65 °C for 10 min. RNA purity and concentration was measured using Nanodrop 2000 (Thermo scientific).

**3.11.3 First strand cDNA synthesis**

First-strand cDNA was synthesized by priming total RNA with hexamer random primers (Invitrogen) and using Superscript II reverse transcriptase (Invitrogen), which is an engineered version of Moloney Murine Leukemia Virus RT with reduced RNase H activity and increased thermal stability. This enzyme can be used to generate cDNA up to 12.3kb.

Total RNA	3 $\mu$ g
Random primer (250 ng/ $\mu$ l)	1 $\mu$ l
dNTP mix 10 mM each)	1 $\mu$ l
Nuclease-free water	To a final volume of 12 $\mu$ l

Heat the mixture to 70 °C for 5 min and quick chill on ice for 2min.

And then add:

5x First-strand buffer	4 $\mu$ l
0.1 M DTT	2 $\mu$ l
Mix contents gently. Incubate at 25 °C for 2 mins.	
Add 1 $\mu$ l (200 units) Superscript TM III and mix gently.	
Incubate at 25 °C for 10 min and 45 °C for 50 mins.	
Inactivate the reaction by heating at 70 °C for 15 mins.	

The cDNA is ready for use.

### 3.11.4 Real-time quantitative PCR

For quantification of transcription level, real-time quantitative PCR with SYBR green (Roche Applied Science) using the 7500 Fast Real-Time PCR System (Life Technologies). Reaction setup for SYBR green:

Faststart universal SYBR green	10 $\mu$ l
Forward primer 30 microM	0.5 $\mu$ l
Reverse primer 30 microM	0.5 $\mu$ l
ddH <sub>2</sub> O	8 $\mu$ l
cDNA	1 $\mu$ l

7500 Fast Real-time PCR setup:

Purpose	Temp.	Time	Cycles
Initial denaturation	95 °C	10 min	1
Denaturation	95 °C	15 s	
Annealing+extension	60 °C	60 s	40

### 3.12 Statistics

At least, 4 animals were included for gene expression analysis by RT-PCR. Cell and myelin quantifications by IHC for cuprizone treated animals were performed for at least 5 animals/group and 2-3 slides per animal. 6 animals per group were included for chEAE experiments and the corresponding quantifications with 2-3 slides per animal and spinal cord.

All data are given as means  $\pm$  SEM. Statistical differences between various groups were analyzed by one-way analysis of variance (ANOVA) followed by Tukey's post-hoc test. Differences between 2 groups were analyzed by Student's t test. De-remyelination scores were analyzed by nonparametric methods, Kruskal-Wallis or Mann-Whitney tests. Statistical analysis was performed using GraphPad Prism 5 (GraphPad software Inc., USA). Statistical significance was set at  $p < 0.05$ .

## 4 Results

### 4.1 Smpd1 deficiency prevents chEAE symptoms and demyelination

To determine whether acid sphingomyelinase plays a role in chEAE, Smpd1 genetically deficient mice and corresponding WT littermates were immunized with MOG<sub>33-55</sub> and scored daily till 45 days post immunization; symptoms were recorded according to a - scale from 0 to 5 as mentioned in section 3.2.2.3 (Fig.8).

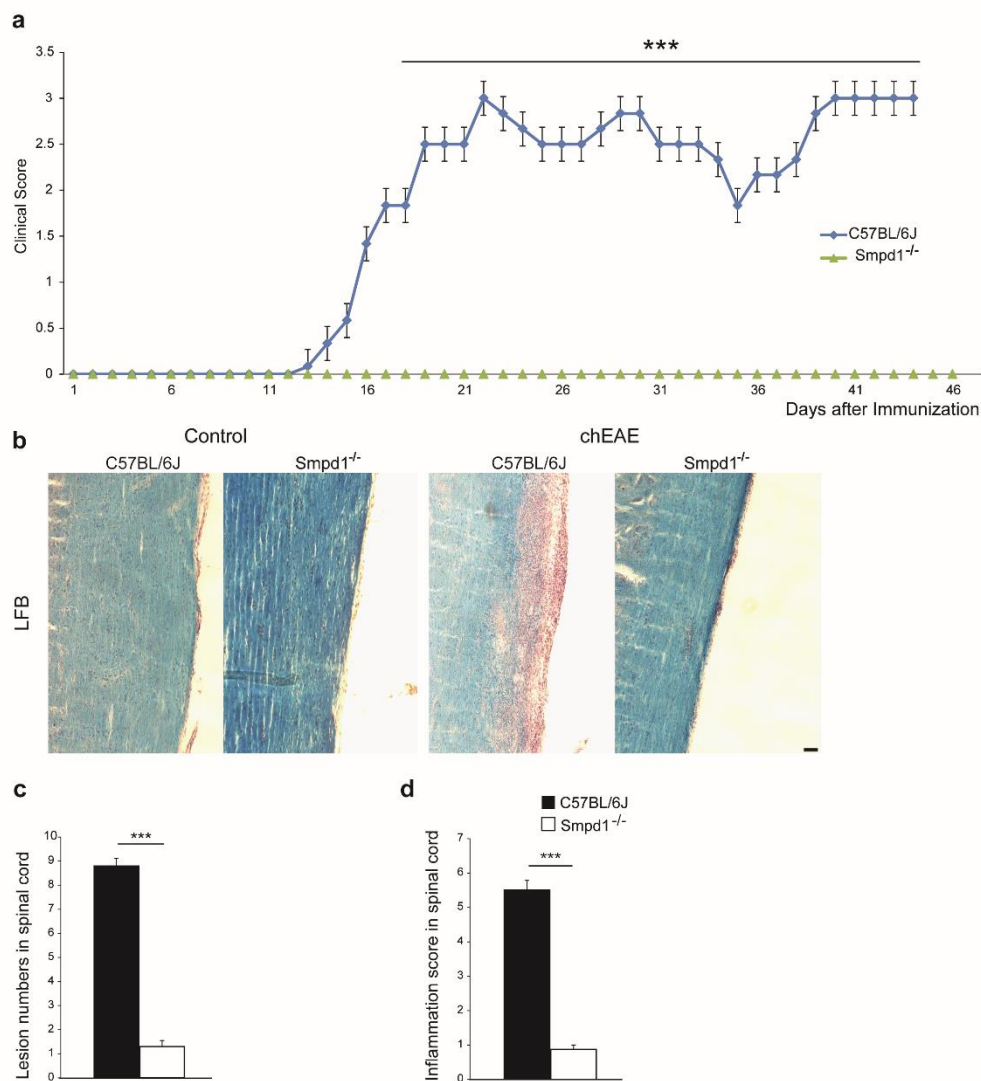


**Figure 6: Genetic Smpd1 deficiency prevents chEAE symptoms and demyelination.** chEAE was induced in Smpd1<sup>-/-</sup> mice and corresponding C57BL/6J wild-type littermates, chEAE symptoms were scored daily on a scale from 0 to 5. Smpd1<sup>-/-</sup> showed no clinical

score compared to wild types (A). LFB staining of the isolated spinal cords after 45 days of disease course revealed that no demyelination or infiltration occurred in Smpd1<sup>-/-</sup> mice compared to wild type animals (B). Lesion numbers and inflammation score was recorded, a significant difference was observed between Smpd1<sup>-/-</sup> and wild-type mice (C). \*\*\*p<0.001 Smpd1<sup>-/-</sup> vs wild-type . Scale bar 50 µm.

Smpd1 genetically deficient mice showed no chEAE symptoms through the 45 days duration post immunization with a clinical score of 0 during the whole studied period. On the other hand, wild-type littermate mice got sick and showed disease symptoms during the same duration with a clinical score ranging between 0.5 and 3.

To investigate the degree of demyelination, spinal cord sections were stained using luxol fast blue and revealed no demyelination in Smpd1<sup>-/-</sup> mice compared to wild-type littermates. To assess lesion numbers and inflammation a scoring system was applied as detailed in section 3.7. Smpd1<sup>-/-</sup> mice showed a significantly lower number of lesions and inflammation score compared to chEAE wild-type littermates (**Fig. 8c and 8d**).

As negative controls, spinal cords isolated from both Smpd1<sup>-/-</sup> and wild-type mice without chEAE induction demonstrated no lesions and no inflammation.

## 4.2 T cell infiltration to the CNS is inhibited by Smpd1 deficiency

Demyelination and neurodegeneration in MS are direct causes of inflammatory activation (Henderson et al., 2009), based on that at day 45 post immunization Smpd1<sup>-/-</sup> and corresponding wild-type littermates were sacrificed and IHC against CD3 was performed to investigate the effects of Smpd1<sup>-/-</sup> on neuroinflammatory activation and T cell recruitment to the CNS (**Fig. 9a**).

Smpd1<sup>-/-</sup> mice significantly inhibited infiltration of T lymphocytes in the spinal cord, as demonstrated by significantly fewer CD3<sup>+</sup> cells in Smpd1<sup>-/-</sup> mice compared to wild-type chEAE mice (**Fig. 9b**).

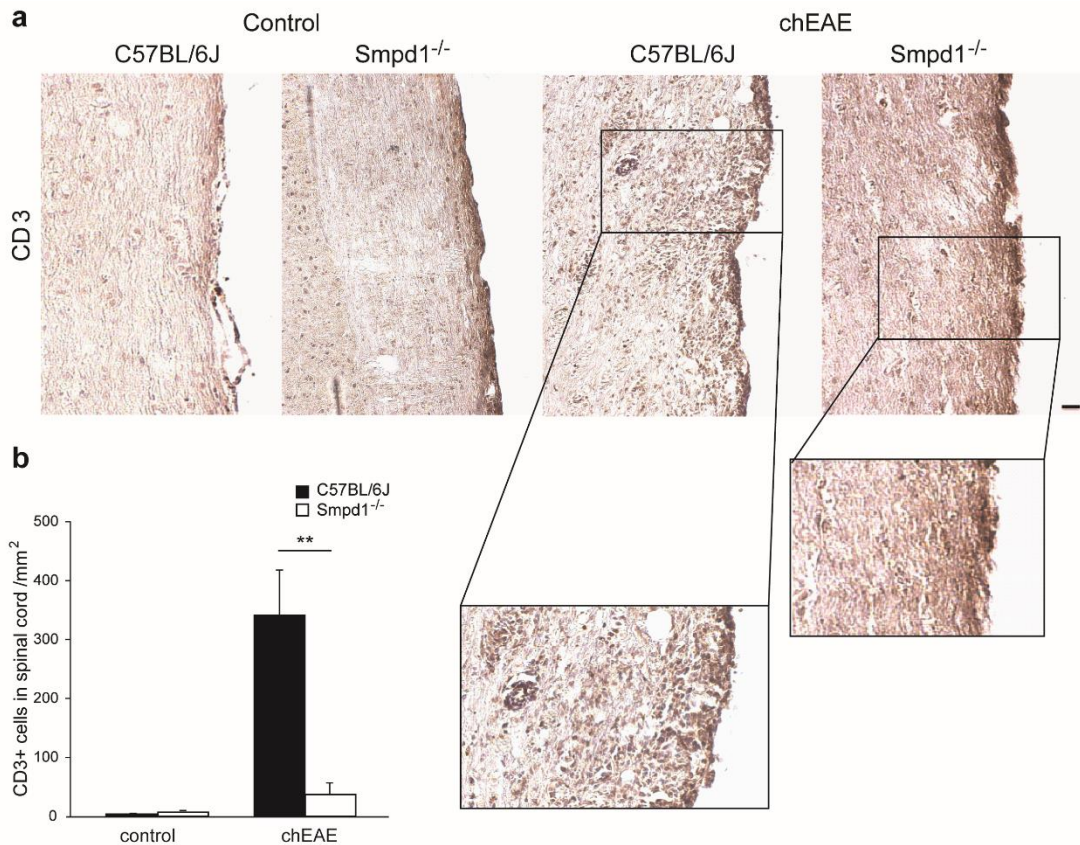


**Figure 7: Genetic Smpd1 deficiency inhibits lymphocyte infiltration to the spinal cord.** chEAE Smpd1<sup>-/-</sup> and C57BL/6J wild-type littermate spinal cord sections stained using IHC against CD3 antibody (A). Smpd1<sup>-/-</sup> mice significantly reduced T cell infiltration into the CNS (B). Negative control not immunized Smpd1<sup>-/-</sup> and wild-type animals show little to none T cells in the spinal cords. \*\*p<0.01 Smpd1<sup>-/-</sup> vs wild-type. Scale bar 50 μm.

### 4.3 Smpd1 deficiency significantly decreases astrogliosis and microgliosis

Reactive astrocytes surround plaques forming astrocytic scars blocking the recovery in MS (Kuhlmann et al., 2008). Microglia as well plays a significant role in the intensity of neuroinflammation (Heppner FL et al., 2005).

IHC, antibodies against GFAP and Iba-1 markers for astrocytes and microglia respectively (**Fig. 10a**) were applied to study the effect of Smpd1 deficiency on astrogliosis and microgliosis in chEAE. Cell count was performed in spinal cord of chEAE animals, Smpd1<sup>-/-</sup> mice showed a significant decrease in both astro-

gliosis and microgliosis compared to wild-type chEAE littermates (Fig. 10b and 10c).

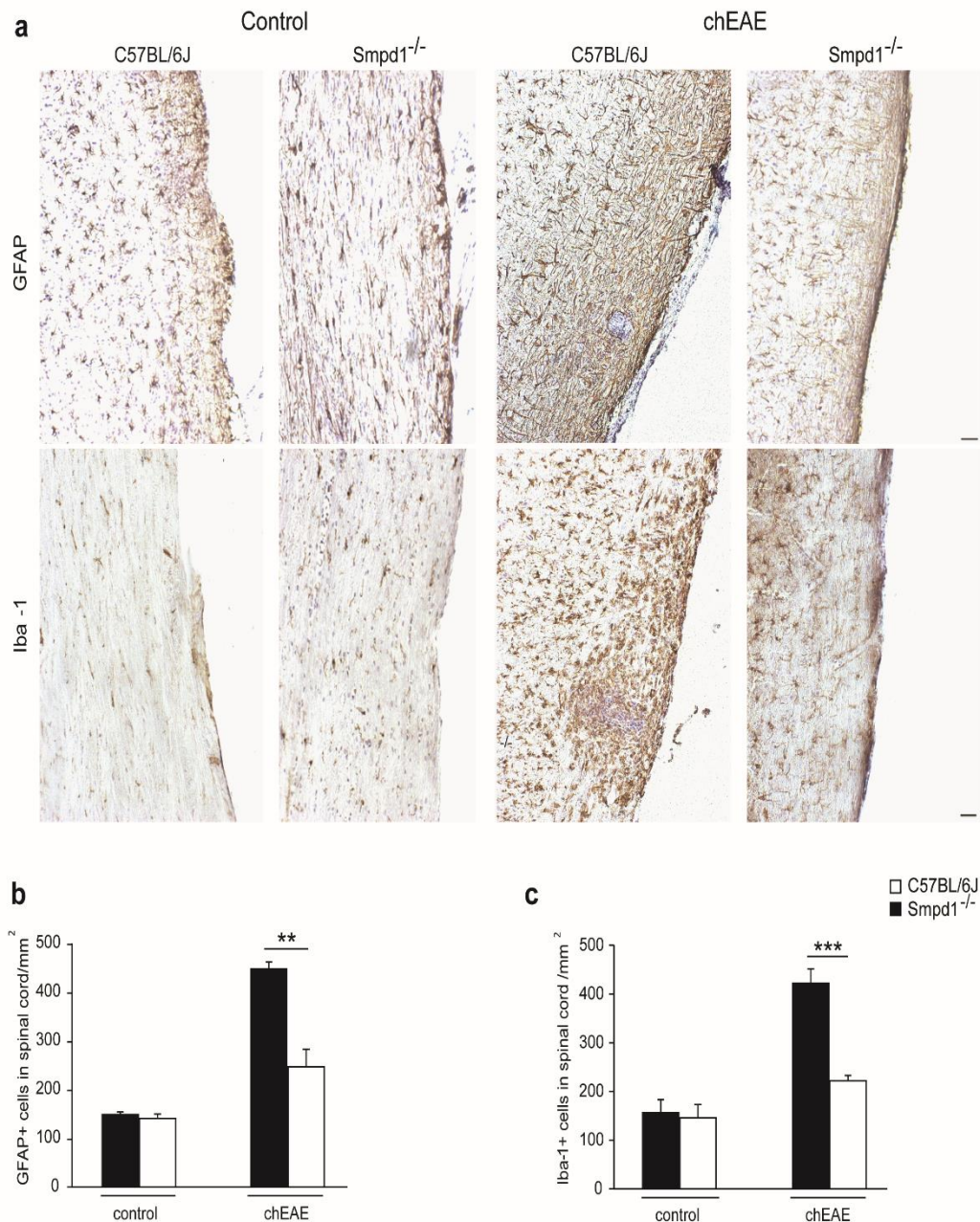


**Figure 8: Smpd1 deficiency significantly decreases astroglia and microglia in chEAE compared to C57BL/6J littermates. Spinal cord histopathology was performed at day 45 of chEAE using antibodies against GFAP and Iba-1. Wild-type chEAE mice showed a significantly higher number of astrocytes and microglia in the spinal cord compared to chEAE Smpd1<sup>-/-</sup> animals (A). GFAP<sup>+</sup> and Iba-1<sup>+</sup> cells with positive nuclei were counted and quantified in the spinal cords in an area not less than 11x10<sup>6</sup> μm. Both GFAP<sup>+</sup> and Iba-1<sup>+</sup> cell number were significantly lower in Smpd1<sup>-/-</sup> mice compared to wild-type (B). \*\*\*p<0.001 and \*\*p<0.01 Smpd1<sup>-/-</sup> vs wild-type. Scale bar 50 μm**

#### 4.4 Pharmacological inhibition of ASM by amitriptyline attenuates chEAE symptoms, astrogliosis and microgliosis

As a potential therapeutic option, we studied whether the inhibition of ASM using amitriptyline would reveal same results as genetic *Smpd1* deficiency. Wild-type chEAE mice and corresponding littermates were treated with amitriptyline or PBS at the detection of weight loss, days 12-14 post immunization for 6 days in a bi-daily manner. chEAE animals were scored daily during the duration of the 45 days, a significant attenuation of chEAE symptoms was observed after the inhibition of ASM in amitriptyline treated animals compared to mice receiving only PBS (Fig. 11a).

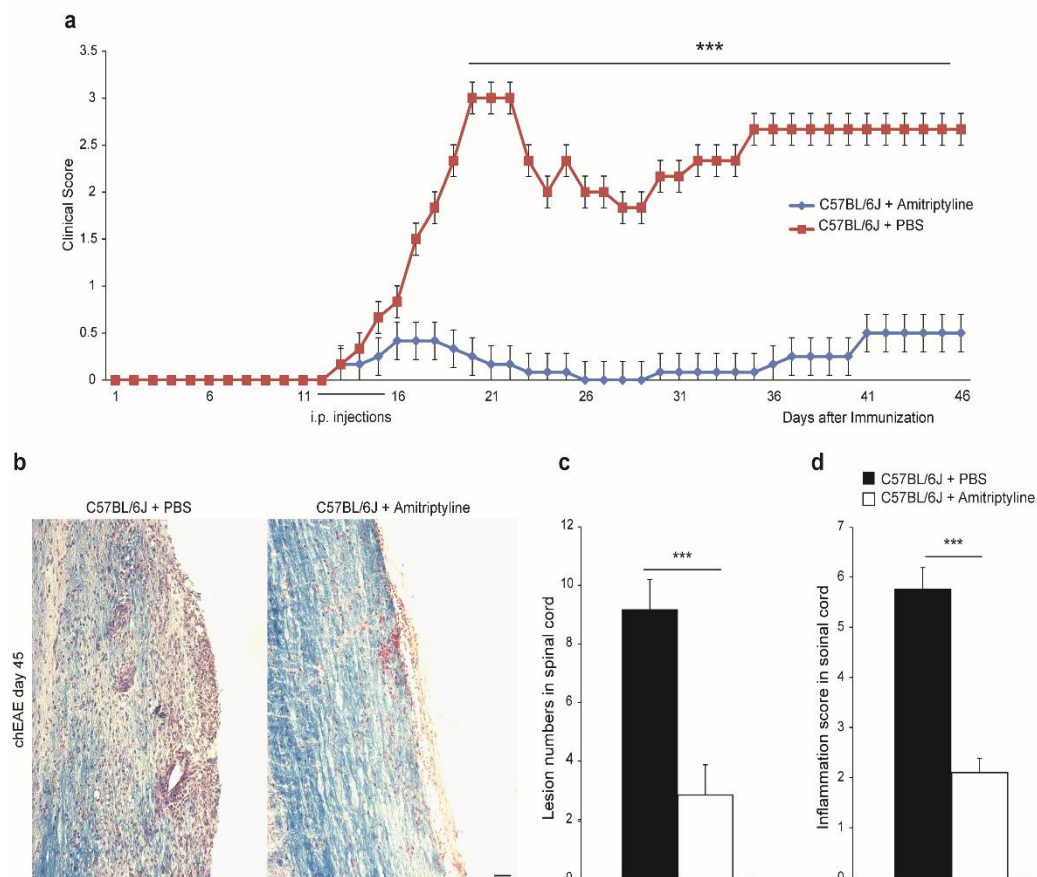


**Figure 9: Pharmacological inhibition of ASM significantly decreases chEAE symptoms and demyelination. C57BL/6J and corresponding littermates were immunized, treated with amitriptyline or PBS as control, and scored for chEAE symptoms till day 45. Amitrip-**

tyline treatment significantly attenuated chEAE compared to animals treated with PBS (A). The inhibition of ASM by amitriptyline showed a significant decrease in lesion number and inflammation score compared to control, observed in LFB stained spinal cord section at day 45 of chEAE (B and C). \*\*\* $p < 0.001$ , amitriptyline treated vs PBS Wild-type. Scale bar 50  $\mu\text{m}$ .

LFB staining revealed significant decrease in both lesion numbers and inflammation score in the amitriptyline treated groups compared to PBS treated animals (Fig. 11b, 11c and 11d).

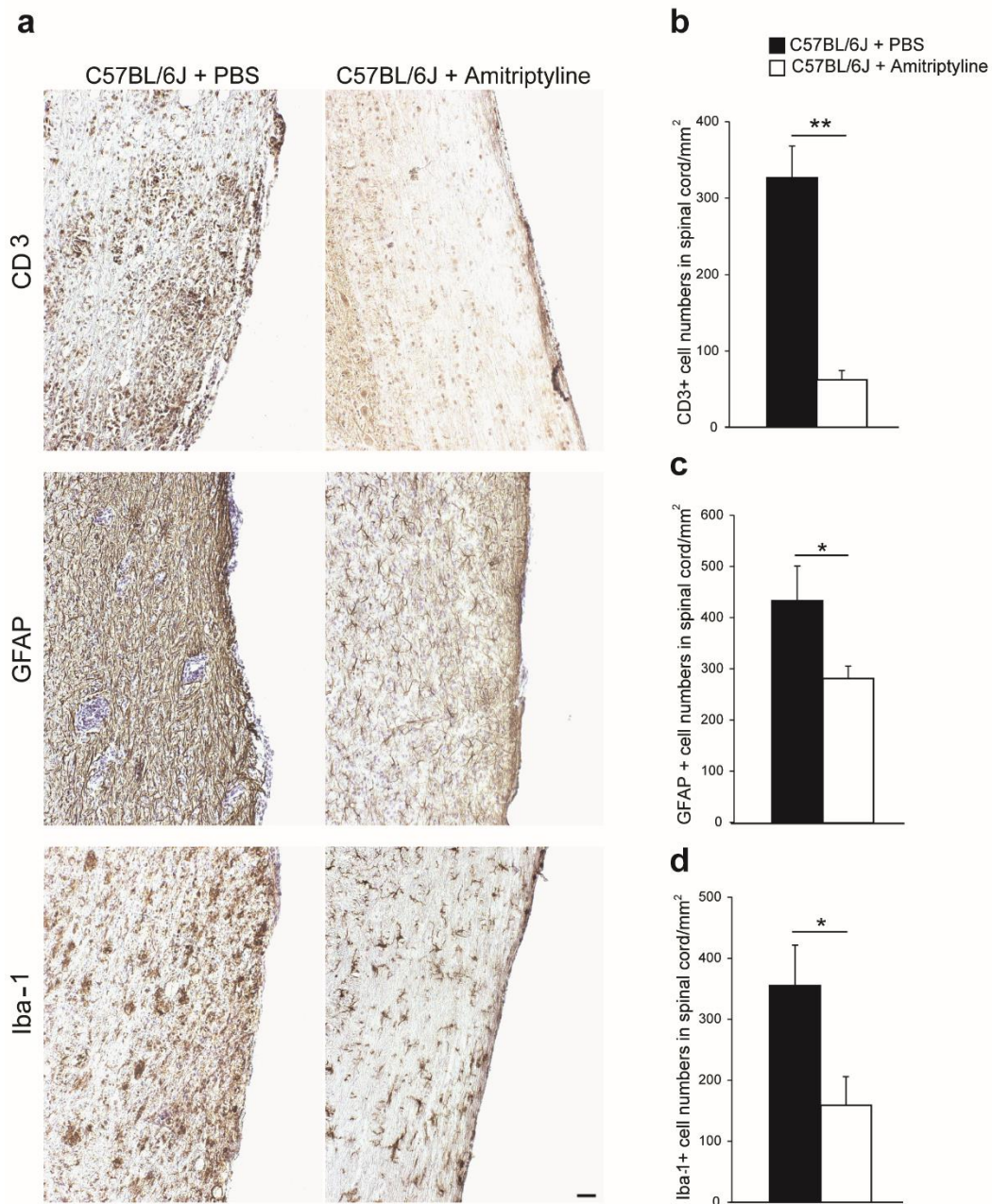


Figure 10: ASM inhibition by amitriptyline stops T cell infiltration and significantly lowers astrogliosis and microgliosis in chEAE. At day 45 of chEAE spinal cords from C57BL/6J amitriptyline treated and controls, were isolated, processed and stained against CD3 (T-

cells), GFAP (astrocytes) and Iba-1 (microglia) (A). Positive cells with visible nuclei were counted and quantified (B). Inhibition of ASM by amitriptyline significantly decreased T cell infiltration to the CNS compared to PBS controls as demonstrated by CD3<sup>+</sup> cell numbers in the spinal cords of chEAE mice. Astrogliosis and microgliosis in amitriptyline treated chEAE animals were significantly lower compared to PBS treated wild-types chEAE mice. \*\*p<0.01 and \*p<0.05 amitriptyline treated chEAE vs PBS chEAE wild-types. Scale bar 50  $\mu$ m

Immunohistochemistry against CD3 was used for the detection of lymphocyte infiltration in the spinal cord of chEAE mice and revealed a significant decrease in T cell infiltration after the inhibition of ASM compared to PBS treated chEAE animals (**Fig. 12a and 12b**).

ASM inhibition by amitriptyline not only lowered T cell numbers in the spinal cord of chEAE mice, but also significantly decreased neuroinflammation in the CNS demonstrated by lower astrocyte and microglia numbers (**Fig. 12c and 12d**).

Negative control animals not immunized and untreated showed no T cell infiltration to the spinal cord nor astrogliosis or microgliosis.

### 4.5 Smpd1 deficiency enhances myelin recovery after acute and chronic demyelination

Cuprizone treatment for 5 (acute) or 12 (chronic) weeks causes significant demyelination with the potential to recover after drug deprivation. In order to investigate the role of Smpd1 in this process, the extend of demyelination was

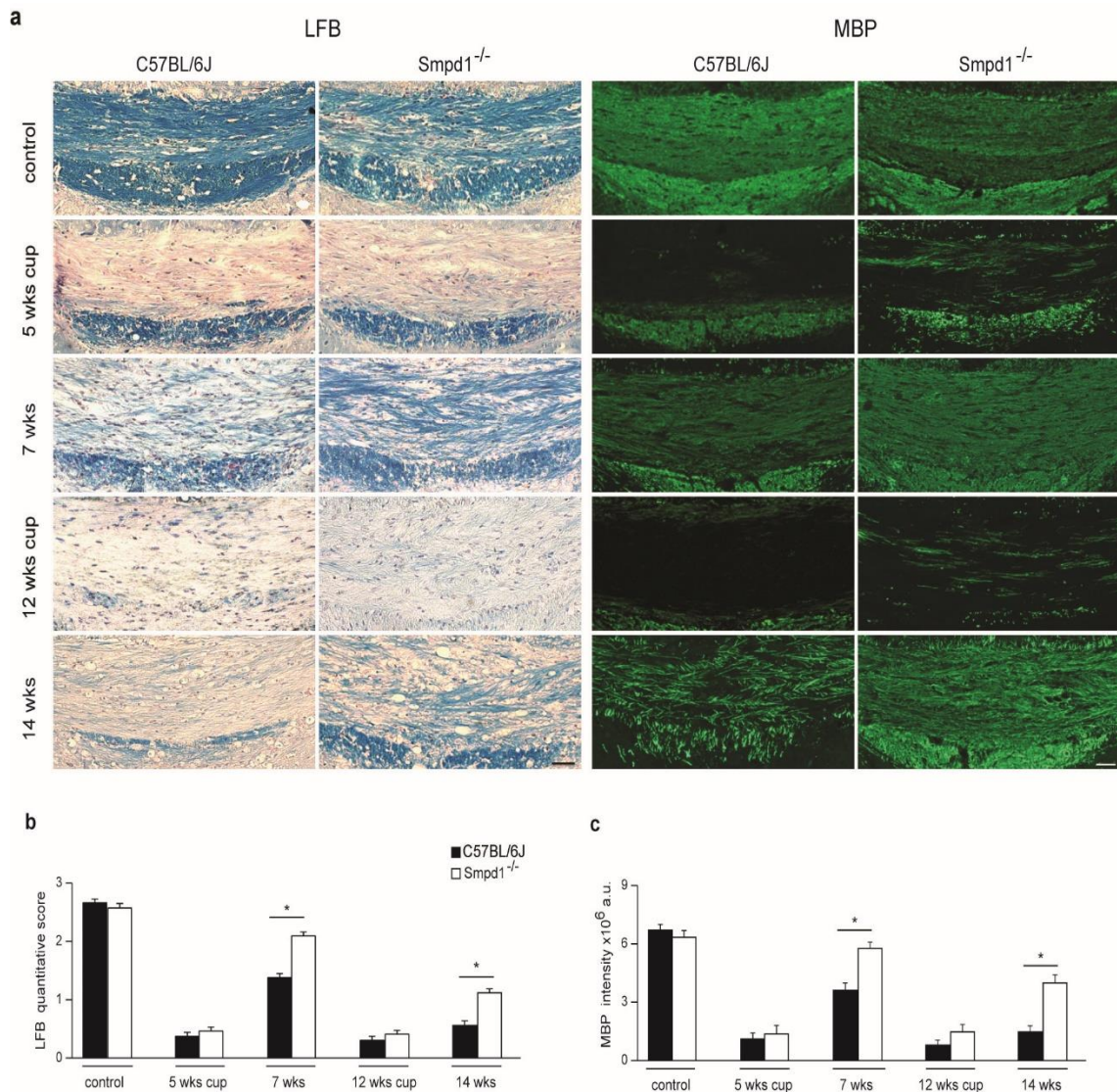


**Figure 11: Brain sections were stained for LFB and MBP. Cuprizone treatment for 5 weeks or 12 weeks causes a massive decrease in myelination as determined by LFB and MBP staining in the CCm (a). Smpd1<sup>-/-</sup> mice showed a significant remyelination compared to C57BL/6J wild-type littermates after 2 weeks of recovery period weeks 7 and 14, determined by the quantification of myelination score (b) and MBP fluorescence intensity in the CCm (c). \*p<0.05 Smpd1<sup>-/-</sup> vs wild-type remyelination weeks 7 and 14. Scale bar, 100 μm.**

immunohistochemically displayed by LFB-PAS and myelin basic protein staining (**Fig. 13a**) and of axonal damage by APP and synaptophysin analysis (**Fig. 14**) in the midline of the corpus callosum (CCm), one characteristically affected brain region in the cuprizone mouse model (Kuhlmann et al., 2002; Skripuletz et al., 2012; Kipp et al., 2009; Pfeifenbring et al., 2015). *Smpd1* deficiency significantly restored myelin formation after a 2 week recovery phase following acute- and chronic cuprizone treatment (**Fig. 13b and 13c**).

In addition, axonal damage was significantly reduced in *Smpd1* deficient mice compared to wild-type littermates, in the recovery phase after acute, but not chronic demyelination (**Fig. 14b and 14c**). Olig-2 is a cellular oligodendrocyte marker, strongly expressed by oligodendrocyte precursor cells (OPCs) and only weakly by mature oligodendrocytes (Kuhlmann et al., 2008).

Corresponding to the previous data, a significant increase in oligodendrocytes proliferation was detected after recovery from both, acute and chronic cuprizone treatment in the CCm of *Asm* deficient animals compared to wild-type mice (**Fig. 14e and 14d**).

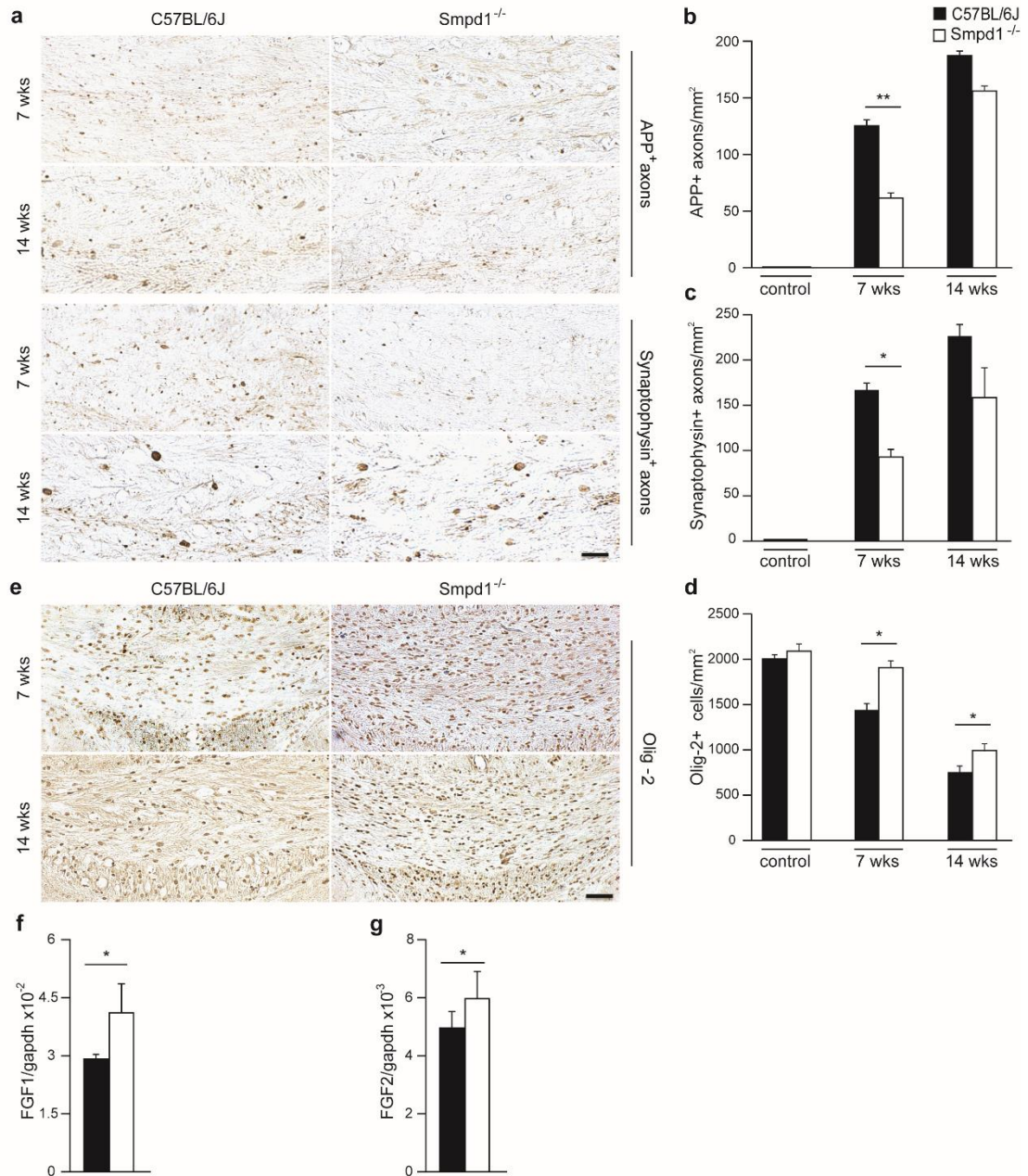


**Figure 12 : Axonal damage analysis with IHC. Staining for APP and synaptophysin in the CCM of wild-type and Smpd1<sup>-/-</sup> animals after acute or chronic cuprizone treatment followed by 2 weeks recovery period week 7 and week 14 respectively (a). Smpd1<sup>-/-</sup> mice showed significantly lower damaged axons in the acute treated groups followed by 2 weeks remyelination compared to wild-type mice (b, c). This difference was not significant after the 12 weeks treatment of cuprizone followed by 2 weeks recovery period. \*\* p < 0.01 and \* p < 0.05 Smpd1<sup>-/-</sup> vs wild-type. Scale bar, 50 μm. IHC revealed a significant increase in Olig-2+ cell numbers in Smpd1<sup>-/-</sup> mice compared to wild-type after acute or chronic cuprizone treatment followed by 2 weeks recovery period week 7 and 14 respectively (d,e). \* p < 0.05 Smpd1<sup>-/-</sup> vs wild-type. Scale bar, 100 μm. The effect of Smpd1 gene deficiency during the 2 weeks recovery after 5 weeks cuprizone feeding (week 7) on mRNA expression levels of different growth factors was analyzed. FGF1 and FGF2 mRNA levels were significantly increased in Smpd1<sup>-/-</sup> mice compared to wild-type PBS treated (f, g). \* p < 0.05 Smpd1<sup>-/-</sup> vs wild-type**

Myelin growth has been shown to be controlled by fibroblast growth factors (FGF) (Furusho et al., 2012; Mohan et al., 2014). Therefore, FGF-1 and -2 mRNA levels were analysed. Smpd1 deficient mice showed a significant increase of FGF-1 and -2 compared to wild-type littermates after the 2 week recovery phase following acute demyelination, hinting towards improved myelin regeneration (**Fig. 14f and 14g**).

Irrespective, we did not detect any difference in the degree of demyelination or axonal damage direct after 5 or 12 weeks cuprizone treatment without time to recover (**Fig. 13b, 13c and 14b 14c**).

#### **4.6 Smpd1 deficiency reduces astrogliosis and production of inflammatory cytokines after acute demyelination**

Glial cells, especially astrocytes have been discussed to play a dual role in myelin disorders. Beside their synaptic stabilizing function, they can also promote inflammatory reactions with subsequent myelin and axonal damage.

Therefore, we investigated glial cell proliferation by immunohistochemistry and production of respective inflammatory markers by real-time PCR. The result showed a significant reduction in astrocyte cell numbers and astrocytic activation, displayed by GFAP staining intensity, in Smpd1 deficient animals compared to wild-type littermates after the 2 week recovery phase following 5 weeks of cuprizone treatment (**Fig. 15a, 15c and 15d**).

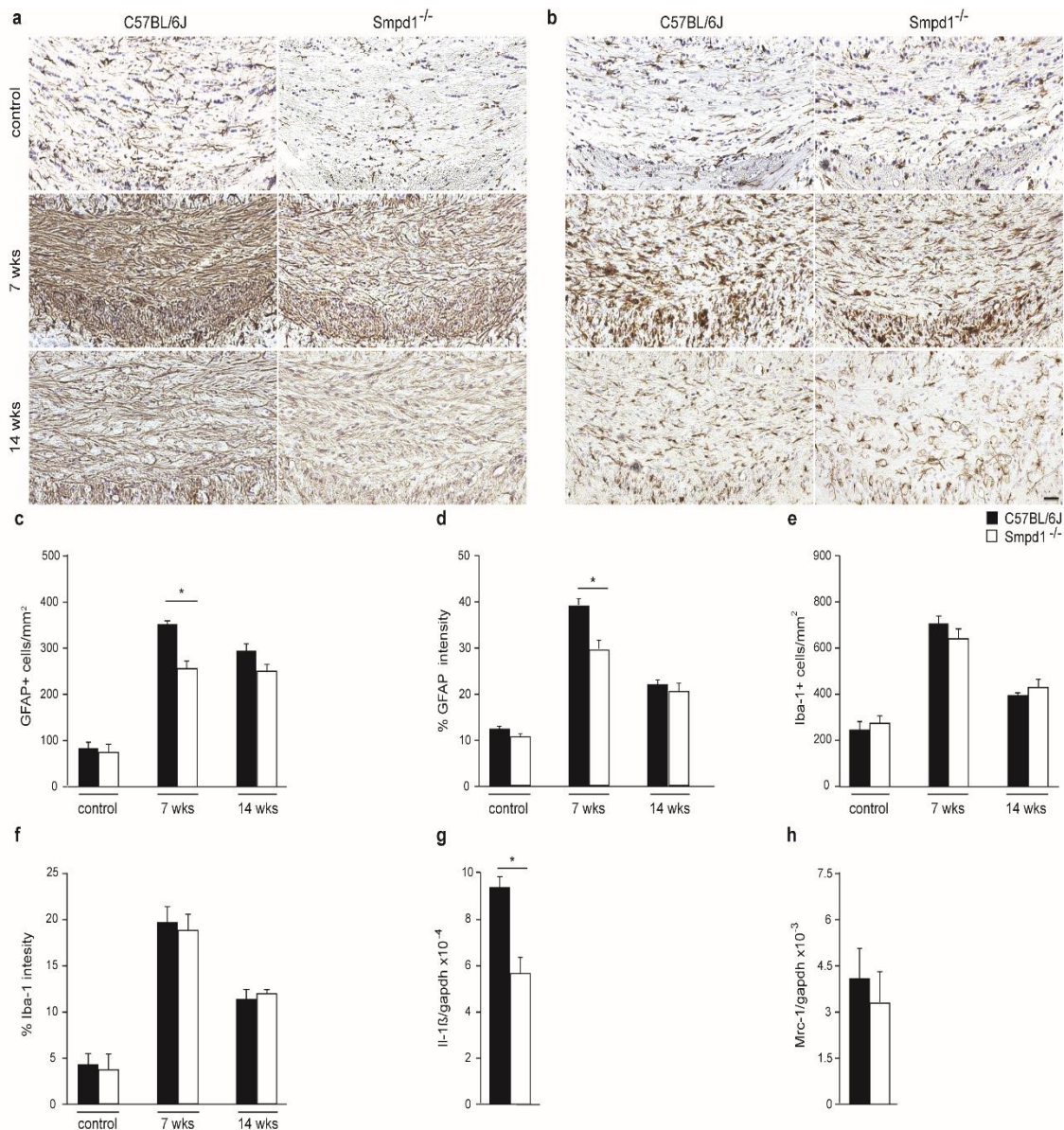


**Figure 13: Effect of *Smpd1*<sup>-/-</sup> on astrogliosis and microgliosis.** The effect of *Smpd1*<sup>-/-</sup> on astrogliosis (a) and microgliosis (b) in the CCm after 5 or 12 weeks cuprizone treatment followed by 2 weeks remyelination. IHC revealed a significant decrease of GFAP+ cells and GFAP staining intensity in *Smpd1*<sup>-/-</sup> compared to C57Bl/6J mice after 5 weeks of cuprizone treatment followed by 2 remyelination, week 7 (c, d). *Smpd1* knockout has no effect on microgliosis neither in acute nor in chronic groups (e, f). \**p*<0.05 *Smpd1*<sup>-/-</sup> vs C57Bl/6J. Scale bar, 100  $\mu$ m. *Smpd1* deficiency significantly decreased Il-1 $\beta$  mRNA expression levels compared to wild-type PBS treated animals (g) after 5 weeks cuprizone treatment followed by 2 weeks recovery. mRNA expression levels of *Mrc-1* showed no significant difference between the compared groups (h). \**p*<0.05 *Smpd1* deficient vs C57Bl/6J wild-types.

This difference was not observable after chronic demyelination (Fig. 15c and 15d). Correspondingly, a significant decrease of pro-inflammatory interleukin-1 $\beta$

(IL-1 $\beta$ ) mRNA levels could be detected in Smpd1deficient animals compared to wild-type littermates (**Fig. 15g**).

As demonstrated in **Fig. 17b, e** and **f**, Smpd1 deficient mice neither showed any difference in the number or staining intensity of Iba-1 positive microglial cells nor in mRNA expression of Mrc-1 (**Fig. 15h**), a marker correlating to anti-inflammatory M2 microglia phenotype (Röszer 2015). Non-cuprizone treated healthy control mice only showed few astrocytes or microglia in the CCm (**Fig. 15c** and **15e**).

#### 4.7 Pharmacological inhibition of ASM as therapeutic option for myelin repair

To elaborate a potential therapeutic approach, the effect of pharmacological inhibition of ASM by amitriptyline was investigated in wild-type littermate mice in

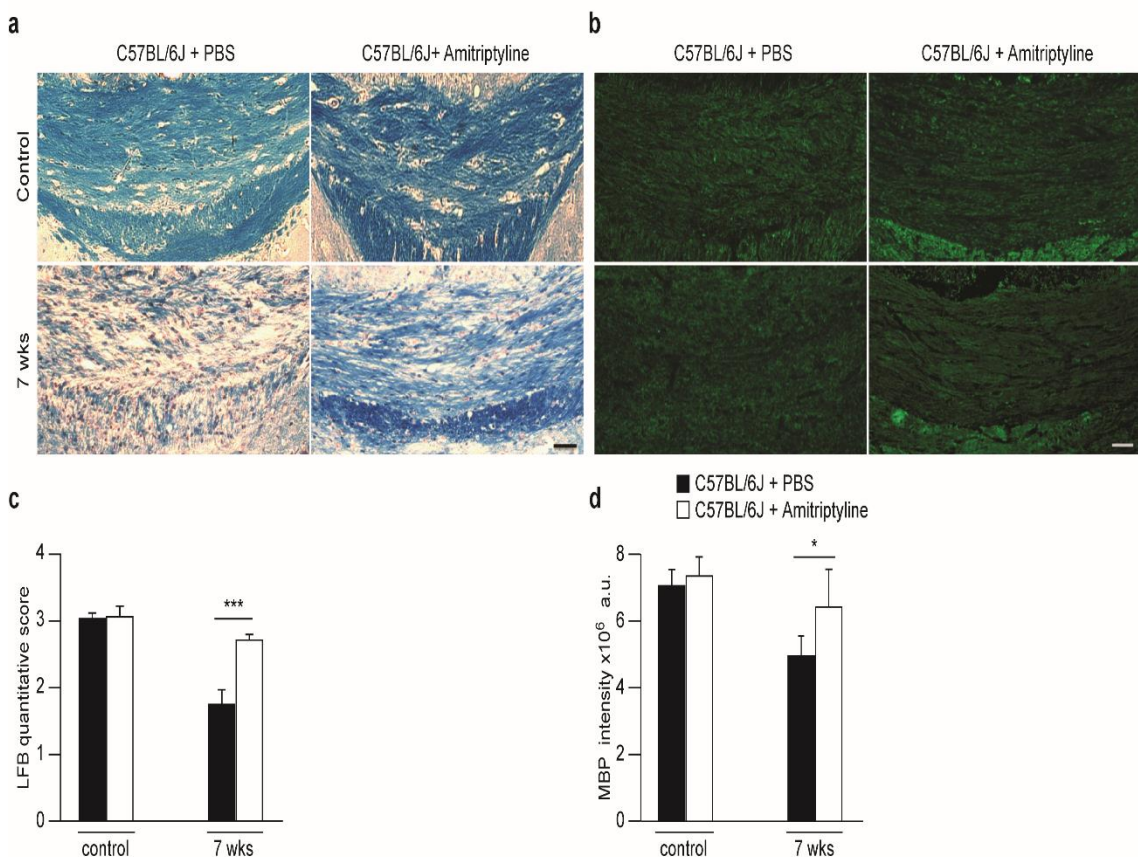


**Figure 14: Brain sections stained for LFB and MBP.** The representative brain sections stained for LFB (a) and MBP (b) are shown in the CCm of control and amitriptyline treated

mice. The extent of de- and remyelination was judged by scoring LFB stained brain section and quantifying MBP intensity of the CCm in control and treated animals. The inhibition of ASM by amitriptyline significantly restored myelin compared to PBS treated animals after 5 weeks cuprizone treatment followed by 2 weeks of recovery (c, d).\*\*\*p<0.001 and \*p<0.05 Amitriptyline treated vs PBS. Scale bar, 100  $\mu$ m.

the acute cuprizone model. Therefore, 5 week cuprizone treatment was followed by the 2 week recovery period, during which amitriptyline injections or PBS injections were administered twice daily.

The inhibition of ASM by amitriptyline showed a significantly higher myelin recovery in the CCm compared to animals treated with PBS as revealed by LFB and MBP intensity (**Fig. 16**). Axonal damage in the CCm of animals treated with amitriptyline was significantly decreased compared to PBS treated mice (**Fig. 17a, 17b and 17c**) as assessed by APP positive neurons and synaptophysin positive buds.

Concerning the groups mentioned in *section 3.2.3*, the differences between *Smpd1*<sup>-/-</sup> and C57BL/6J wild-type littermate mice in the 5 weeks demyelination groups and the 1 week remyelination were not significantly different (data not shown).

In addition, Olig-2<sup>+</sup> cell numbers in amitriptyline-treated animals were significantly increased compared to the PBS treated mice after 2 weeks of recovery (**Fig. 17d and 17e**) and myelin growth factors FGF-1 and -2 showed an increased mRNA level after amitriptyline treatment (**Fig. 17f and 17g**).

Untreated control animals did not show any APP or synaptophysin positive buds, no axonal damage was observed (**Fig. 17b and 17c**).

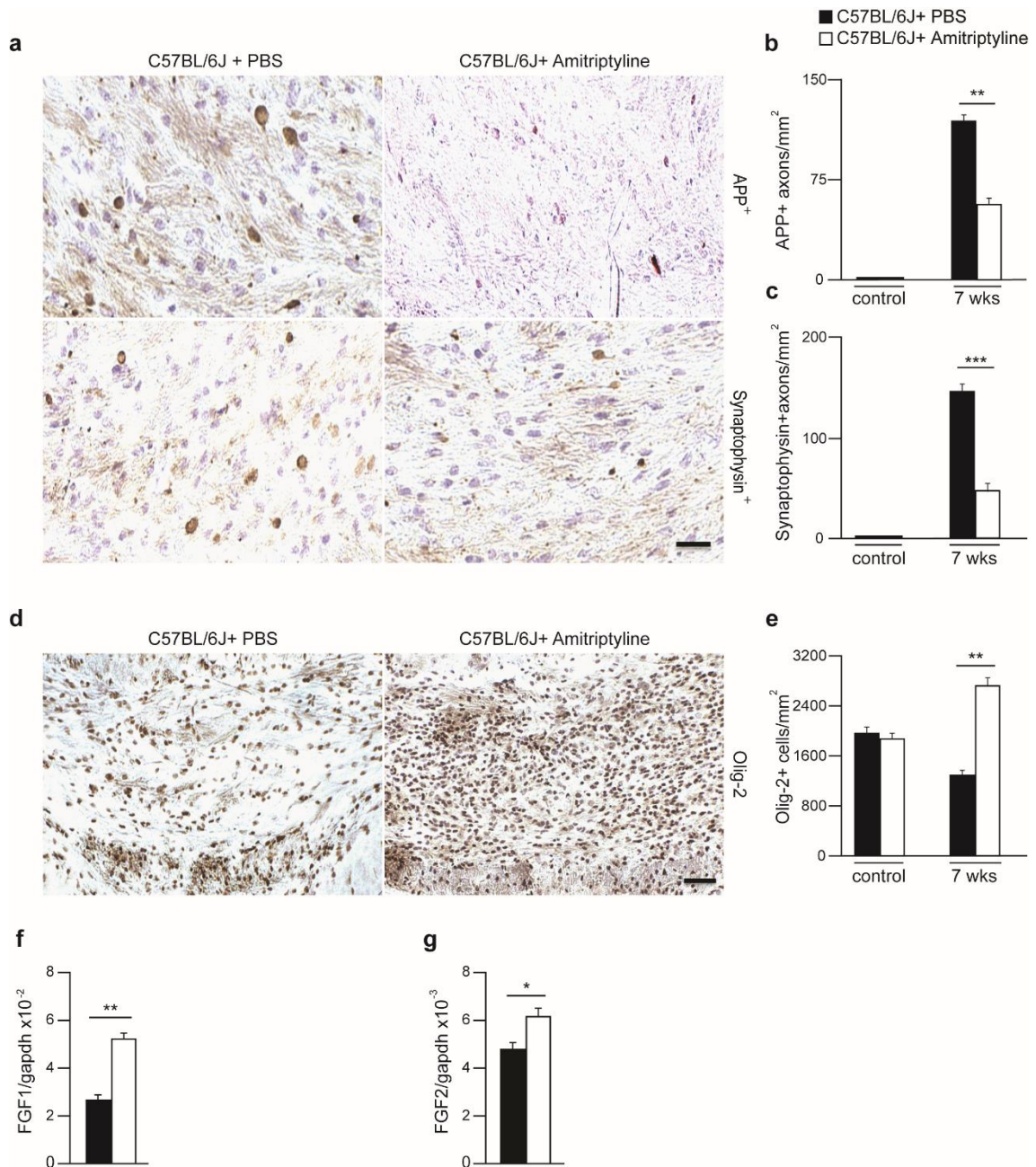


**Figure 15: Stainings for APP and synaptophysin IHC staining for APP and synaptophysin in the CCm of amitriptyline or PBS treated animals during the 2 weeks recovery after 5 weeks of cuprizone treatment (a). ASM inhibition by amitriptyline showed significantly lower axonal damage, as demonstrated by APP and Synaptophysin positive buds in the CCm (b, c). \*\* $p < 0.01$  and \*\*\* $p < 0.001$  amitriptyline treated vs PBS treated mice. Scale bar, 50  $\mu\text{m}$ . IHC revealed a significant increase of Olig-2+ cells in the CCm of amitriptyline treated mice compared to PBS treated (d, e). mRNA expression levels of FGF-1 and FGF-2 mRNA levels were significantly increased in amitriptyline treated mice compared to PBS controls (f, g). \*\* $p < 0.01$  and \* $p < 0.05$  amitriptyline treated vs PBS treated.**

Corresponding to previous results, one effect of ASM inhibition by amitriptyline was a reduction of the detrimental astrocytosis. Amitriptyline mice showed a significant reduction in astrocyte cell numbers and GFAP staining intensity in

the CCm compared to PBS treated animals (**Fig. 18c and 18d**) as well as significant lower levels of the inflammatory cytokines IL-1 $\beta$  (**Fig. 18g**). Again, there was no difference in microglial cell numbers (**Fig. 18e and 18f**).

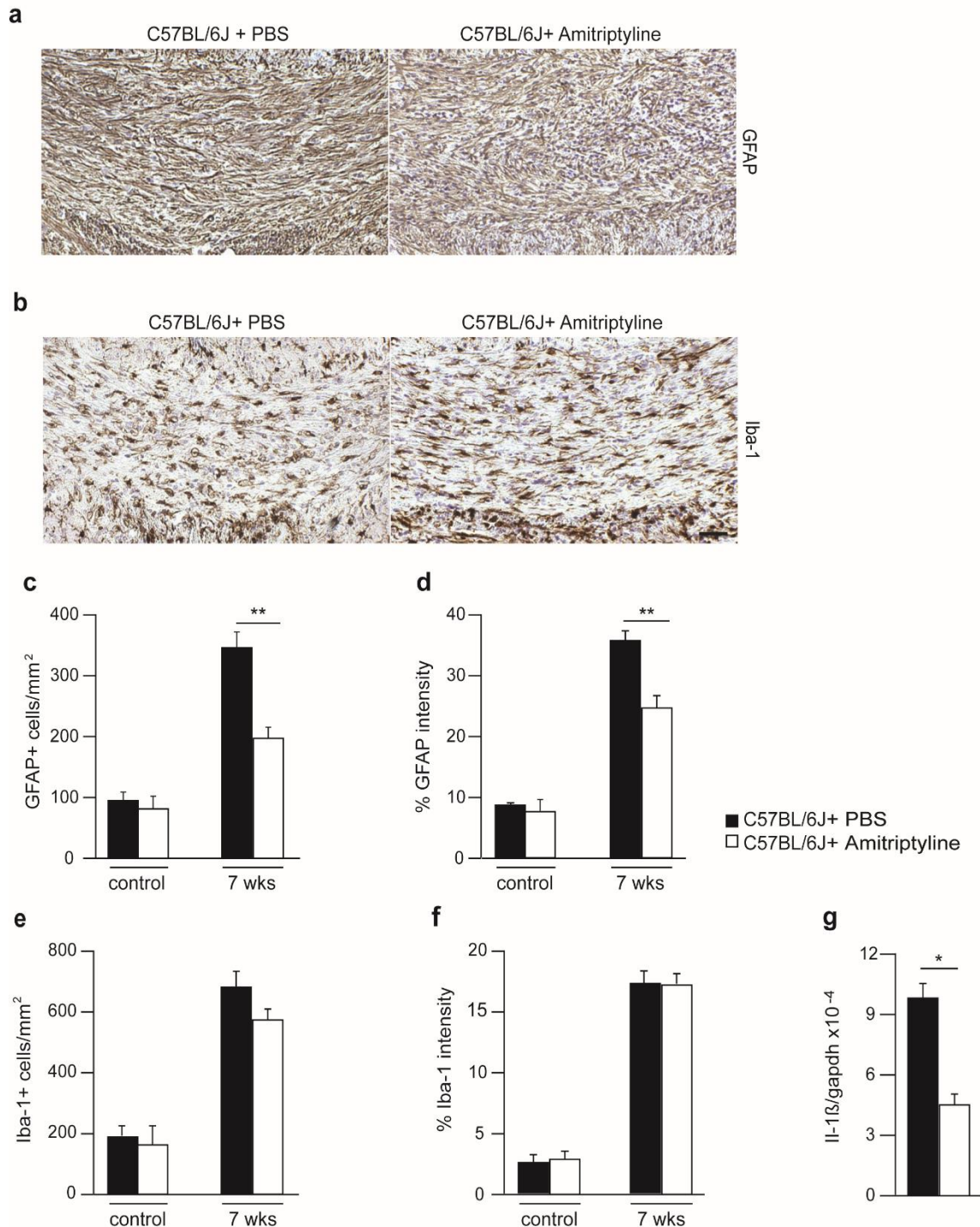


**Figure 16: Astrogliosis and microgliosis after amitriptyline treatment.** ASM inhibition by amitriptyline for 2 weeks of recovery period after 5 weeks cuprizone feeding effects astrogliosis and microgliosis in the CCm (a,b). IHC revealed a significant decrease of GFAP+ cells and GFAP staining intensity of the CCm in the amitriptyline treated group compared to PBS treated (c, d). Iba1 + cell numbers and iba1 staining intensity in the CCm of amitriptyline or PBS treated animals showed no significance difference (e, f).

**\*\*p<0.01 amitriptyline treated vs PBS treated groups. Scale bar, 100  $\mu$ m. The Inhibition of ASM by amitriptyline did significantly decrease Il-1 $\beta$  mRNA expression levels compared to wild-type PBS treated animals during the 2 weeks recovery after 5 weeks cuprizone treatment (g), while mRNA expression levels of Mrc-1 showed no significant difference between the compared groups (h). \*p<0.05 amitriptyline treated vs PBS treated mice.**

## 5 Discussion

MS is a chronic inflammatory disease of the CNS characterized by inflammatory infiltrates, demyelination and axonal loss. It is the most frequent cause of neurological disability in young adults (Lassmann et al., 2011). The invasion of lymphocytes leads to a subsequent myelin loss, astrocyte and microglia activation and oligodendrocyte apoptosis. Recovery and remyelination are challenged by several factors such as the blockage of the proliferation and differentiation of OPCs required to repair damaged myelin (Gudi et al., 2014).

In this study, we demonstrate that genetic or pharmacological inhibition of acid sphingomyelinase activity protects against chEAE, lowering lymphocyte infiltration to the CNS, glia activation and neuroinflammation. Also, Smpd1 deficiency enhances myelin repair after acute or chronic experimental demyelination by lowering astrocytosis and with a significant increase of oligodendrocyte proliferation. Thus, acid sphingomyelinase plays a crucial role in the pathophysiology of MS both acting on T cell transmigration and enhancing remyelination by indirect effect on astrocytes and increased oligodendrocyte proliferation and differentiation. Thus, the ASM/ceramide system can enhance remyelination and recovery after cuprizone induced demyelination.

### 5.1 Acid sphingomyelinase deficiency in chEAE pathophysiology

The sphingomyelin pathway is crucial for maintaining cell integrity and cell function. Enzymes involved in this pathway like acid sphingomyelinase are present throughout the brain. The present study indicates a strong link between acid sphingomyelinase and the pathogenesis of MS. In MS as well as in a chEAE model, autoimmune reactive T cells from the periphery invade the CNS leading to neuroinflammation, demyelination and neurodegeneration (Lassmann et al., 2011).

In this study, we showed that *Smpd1* deficient mice showed attenuated chEAE symptoms accompanied with lower neuroinflammatory activation. In contrast, chEAE wild-type littermates were consistently sick showing significantly higher clinical scores. ASM and its enzymatic product ceramide have both been shown to be highly expressed in active human MS lesion (van Doorn et al., 2010) reporting a role of ASM in MS pathology. We documented that mice lacking clinical disease scores were also free from inflammatory infiltrates, correlating histology results with clinical score. Inflammation and lesion formation is strongly correlated with disease severity (Recks et al., 2011). We demonstrated with CD-3 immunostaining that *Smpd1* deficient mice showed significantly lower number of T cells in the CNS of chEAE animals, pointing toward a direct role of *Smpd1* activity in T cell infiltration in chEAE. These results suggest an important role of the ASM/ceramide system in the development of chEAE and leukocyte infiltration to the CNS. This corresponds to the study by Lopes et al. (2016), reporting *Asm* expression in inflamed brain vasculature and the role of ASM in transmigration process of T cells into the CNS under inflammatory conditions like MS. Lopes et al., suggested that ASM activity controls proper ICAM-1 clus-

tering, hence providing a perfect actin network across which T cells can adhere and transmigrate invading the CNS.

Reactive astrocytes surround plaques forming astrocytic scars blocking recovery in MS. Microglia has a significant role in the intensity of neuroinflammation (Kuhlmann et al., 2008; Heppner et al., 2005). Cell counts for both GFAP and iba-1 markers of astrocytes and microglia respectively, were significantly lower in immunized *Smpd1* deficient mice compared to wild-type littermates. The inhibition of *Smpd1* activity stops T cell infiltration to the CNS, which in turn could affect the degree of neuroinflammation consisting of astrocyte and microglia activation.

### **5.2 Pharmacological inhibition of ASM in chEAE**

Amitriptyline, as well as other functional inhibitors of acid sphingomyelin (FIAS-MA's) drugs, acts by competitive inhibition of ASM (Kornhuber et al., 2010). It inhibits around 60% to 80% of ASM activity (Teichgraber et al., 2008; Beckmann 2014). In this study we show that treatment with amitriptyline significantly reduces clinical scores in chEAE animals, consisting with our results in *Smpd1* genetically deficient mice. Amitriptyline reduced T cell infiltration to the CNS demonstrated by CD-3 staining; in addition cell counts for astrocytes and microglia were significantly lower compared to PBS treated chEAE mice. Our data suggest that amitriptyline inhibition of ASM activity corresponds to the results found in *Smpd1* genetically deficient mice with lower neuroinflammation and glial activation. Thus, given the long-term experience and clinical safety of amitriptyline and the present results in chEAE, amitriptyline could be a promising candidate for MS patients. A clinical study of MS patients treated with fluoxe-

tine, another FIASMA, has already shown a reduction in MRI lesion progression (Mostert et al., 2008; Davies, 2013).

### **5.3 Acid sphingomyelinase deficiency in de- and remyelination**

The results of this study demonstrate that genetic deficiency or pharmacological inhibition of the Asm/ceramide system can enhance myelin repair after cuprizone induced demyelination. By deficiency of the Asm/ceramide system, we could observe a significantly improved recovery of myelin as indicated by MBP and LFB intensity scores and an increase in oligodendrocyte proliferation as indicated by increased Olig-2 positive cells in the recovery phase after cuprizone treatment. This led to a reduction of neuronal damage. Interestingly, MBP/LFB levels and Olig-2 positive cell numbers were close to normal values of completely untreated mice. This is in accordance with the observation that ceramide has been shown to induce oligodendrocyte cell death together with the pro-inflammatory cytokine tumor necrosis factor alpha in human MS brains. In addition, overexpression of ASM and subsequent increase of ceramide resulted in reduced neuronal survival even without any further cell stress (Kim Hye et al., 2011; Kim SunJa et al., 2012; Gulbins et al., 2013).

Fibroblast growth factors are important drivers of myelination (Mohan et al., 2014; Furusho et al., 2012; Messersmith et al., 2000). Further supporting the beneficial effect of ASM/ceramide deficiency, FGF1 and FGF2 showed a significant increase in the recovery phase after acute demyelination. Activation of CNS cells, especially astrocytes, is discussed as important mechanism in MS associated de- and remyelination. Astrocytes can show a dual role with either beneficial functions by facilitating e.g. microglial-mediated myelin clearance (T. Skripuletz et al., 2012) or detrimental functions by enhancing inflammatory mye-

lin toxic reactions by e.g. inflammatory cytokine production (Gudi et al., 2014). ASM-induced ceramide is the principle component of ceramide-enriched membrane platforms, which are a pre-requisite for full cell activation facilitating membrane receptor assembling and subsequent intracellular signalling with possible thunder storm of pro-inflammatory mediators (Gulbins and Li, 2006).

In the current study, as consequence of the *Smpd1* genetic deficiency and subsequent reduced ceramide level, a significant reduction of activated astrocytes and the pro-inflammatory cytokine IL-1 $\beta$  could be observed and might act as potential mechanism for the optimized myelin repair. However, astrocyte numbers in *Smpd1* deficient mice are significantly, but only 30%, reduced compared to wild-type littermates. This is important as a complete ablation of astrocytes leads to a deprivation of their beneficial functions (Skipuletz et al., 2013). The observed differences upon *Smpd1* deficiency were seen in the recovery phase after acute demyelination with 5 weeks of cuprizone treatment, hinting towards an involvement of glial cells mainly after acute myelin injury. Recovery after chronic demyelination (12 weeks of cuprizone) resulted in a still increased myelin content and oligodendrocyte proliferation, but did not show a clear glial cell involvement. There was also no difference in the extent of acute or chronic demyelination directly after 5 or 12 weeks of cuprizone treatment, indicating an equal mode of action of cuprizone in both, *Smpd1* genetically deficient mice or wild-type littermates and further demonstrating a relevant effect of the *Asm*/ceramide system in promotion of remyelination rather than augmentation of demyelination.

Microglia are reported to play a supportive role in remyelination (Gudi et al., 2014). In the cuprizone animal model, they act as marker for drug-induced pa-

thology and are increased and activated after cuprizone treatment (Goldberg et al., 2015). Interestingly, we did not see any difference in these increased microglia cell numbers or in their activation in *Smpd1* deficient versus wild-type littermates in the recovery after acute demyelination, excluding any important role of microglia in myelin repair.

### **5.4 Pharmacological inhibition of acid sphingomyelinase and myelin repair**

As potential therapeutic approach to support remyelination, we could show that the positive effect of *Smpd1* deficiency in myelin recovery can be mimicked by treatment with amitriptyline, a well-known pharmacological Acid sphingomyelinase inhibitor (Kornhuber et al., 2010). Amitriptyline treatment was only initiated after cuprizone-induced myelin damage and was able to restore MBP and LFB intensity to normal values after 2 weeks with an even higher than normal level of oligodendrocyte proliferation. Again astrocytes were inhibited as potential mechanism for neuronal repair. These results strongly hint towards a detrimental role of the ASM/ceramide system not during myelin damage but during potential repair mechanisms.

We show that ASM/ceramide deficiency or amitriptyline-induced pharmacological inhibition enhance remyelination after acute and chronic myelin damage. As potential mechanism a reduction in astrocyte proliferation and activation with reduced pro-inflammatory cytokine release, resulting in enhanced oligodendrocyte proliferation and neuronal preservation could be observed.

We show the effects of acid sphingomyelinase genetic deficiency or its pharmacological inhibition in two animal models of MS. In the chEAE animal model, ASM was reported to have a crucial effect on T cell infiltration to the CNS, and

to stop disease severity in chEAE mice, correlating with recent studies conducted *in vitro* (Lopes et al., 2016). Microgliosis and astrogliosis in Smpd1 deficient mice were also significantly decreased in chEAE model; this might be due to the lower and near to none T cell infiltration of the CNS in Smpd1 deficient mice, which in turn did not activate microglia and astrocytes. This observation is in contrast to what was observed in chEAE wild-type mice with a high degree of neuroinflammation. In an effort to translate the corresponding findings, amitriptyline, a known inhibitor of ASM and a widely used anti-depressant, was injected in wild-type chEAE mice. The pharmacological inhibition of ASM corresponded with the results reported in Smpd1 genetically deficient mice. Thus, it might be that ASM-ceramide system would be an important therapeutic target in MS.

In the second animal model of MS, the toxic demyelination model, we wanted to investigate the role of acid sphingomyelinase both in demyelination and as well as in the remyelination phase. During demyelination no results suggested any significant role for acid sphingomyelinase, results showed no significance difference between Smpd1 genetically deficient mice and wild-type mice. In contrast to demyelination, in remyelination we reported a significance difference in myelin repair after two weeks of the cuprizone withdrawal with increased oligodendrocyte proliferation in the Smpd1 deficient mice compared to wild-type littermates.

Hence, our data points towards an important role of acid sphingomyelinase in the remyelination phase both after acute and chronic demyelination. To further investigate and to confirm the role of ASM, we used the functional inhibitor amitriptyline in the 2 weeks recovery phase after cuprizone withdrawal to study

whether the pharmacological inhibition of amitriptyline could yield to similar results as obtained from the Smpd1 deficient mice in the cuprizone model. Amitriptyline injected mice in the recovery phase showed a significant myelin repair compared to mice injected with PBS at the same period and phase of recovery. With results corresponding to the genetic deficiency of Smpd1, increased oligodendrocyte proliferation was documented with a lower degree of astrocyte activation.

Since the BBB remains intact in the cuprizone model we excluded the effect of acid sphingomyelinase on T cells in the toxic demyelination model, and focused our interest on the glial cells. As documented ASM inhibition did significantly decrease astrogliosis in the 2 weeks recovery phase with a higher oligodendrocyte proliferation and differentiation, but did not show any effect on microgliosis. Might be that it is affecting the remyelination pathway which microglia does not have a crucial role in. Certainly, the 30% decrease in astrogliosis compared to that of wild-type has a beneficial effect on remyelination as was suggested before that astrocytes troubles remyelination in chronic MS by inhibiting OPCs proliferation and differentiation. Therefore, the inhibition of acid sphingomyelinase enhanced remyelination by an indirect effect on astrocytes and oligodendrocyte proliferation.

We show that the ASM-Ceramide system plays an important role in T cell infiltration in the chEAE model, stopping disease severity and neuroinflammation reporting the role of ASM on T cell transmigration *in vivo*. Also we report the role of ASM in remyelination showing enhanced myelin recovery after acute and chronic demyelination. With respect to these findings ASM-ceramide system might be a therapeutic option for MS patients.

## 6 References

- Armstrong RC, Le TQ, Frost EE, Borke RC, Vana AC (2002) Absence of fibroblast growth factor 2 promotes oligodendroglial repopulation of demyelinated white matter. *Journal of Neuroscience* 22:8574-8585
- Artemiadis AK, Anagnostouli MC (2010) Apoptosis of Oligodendrocytes and Post-Translational Modifications of Myelin Basic Protein in Multiple Sclerosis: Possible Role for the Early Stages of Multiple Sclerosis. *European Neurology* 63:65-72
- Bakker DA LS (1987) Blood-brain barrier permeability during cuprizone induced demyelination. Implication for the pathogenesis of immune-mediated demyelinating diseases. *J Neurol Sci* 78:125-137
- Barnett MH PJ, Pollard JD, Prineas JW (2009) MS: is it one disease? *Int MS J* 16:57-65
- Beckmann N, Sharma D, Gulbins E, Becker KA, Edelman Br (2014) Inhibition of acid sphingomyelinase by tricyclic antidepressants and analogs. *Frontiers in Physiology* 5
- Bianco F, Perrotta C, Novellino L, Francolini M, Riganti L, Menna E, Soglietti L, Schuchman EH, Furlan R, Clementi E, Matteoli M, Verderio C (2009) Acid sphingomyelinase activity triggers microparticle release from glial cells. *The EMBO Journal* 28:1043-1054
- Blackmore (1972) Observations on oligodendrocyte degeneration, the resolution of status spongiosus and remyelination in cuprizone intoxication in mice. *Journal of Neurocytology* 1: 413-426
- Britta Engelhardt DV, Rupert Hallmann, Martina Schulz (1997) E- and P-Selectin Are Not Involved in the Recruitment of Inflammatory Cells Across the Blood-Brain Barrier in Experimental Autoimmune Encephalomyelitis. *Blood* 90:4459-4472
- Brown GC (2007) Mechanisms of inflammatory neurodegeneration: iNOS and NADPH oxidase. *Biochemical Society Transactions* 35:1119-1121
- Brunkhorst R, Vutukuri R, Pfeilschifter W (2014) Fingolimod for the treatment of neurological diseases state of play and future perspectives. *Frontiers in Cellular Neuroscience* 8
- Bush TG, Puvanachandra N, Horner CH, Polito A, Ostefeld T, Svendsen CN, Mucke L, Johnson MH, Sofroniew MV (1999) Leukocyte infiltration, neuronal degeneration, and neurite outgrowth after ablation of scar-forming, reactive astrocytes in adult transgenic mice. *Neuron* 23:297-308

- Chen H, Tran J-TA, Brush RS, Saadi A, Rahman AK, Yu M, Yasumura D, Matthes MT, Ahern K, Yang H, LaVail MM, Mandal MNA (2012) Ceramide Signaling in Retinal Degeneration. *723:553-558*
- Chhor V, Le Charpentier T, Lebon S, Oré M-V, Celador IL, Josserand J, Degos V, Jacotot E, Hagberg H, Sävman K, Mallard C, Gressens P, Fleiss B (2013) Characterization of phenotype markers and neuronotoxic potential of polarised primary microglia in vitro. *Brain, Behavior, and Immunity 32:70-85*
- Choi JW, Chun J (2013) Lysophospholipids and their receptors in the central nervous system. *Biochimica et Biophysica Acta (BBA) - Molecular and Cell Biology of Lipids 1831:20-32*
- Compston A, Coles A (2002) Multiple sclerosis, Vol 359
- Correale J, Villa A (2009) Role of CD8+ CD25+ Foxp3+ regulatory T cells in multiple sclerosis. *Annals of Neurology:n/a-n/a*
- Davies L (2013) The Role of Acid Sphingomyelinase in Experimental Autoimmune Encephalomyelitis.
- Ferlinz RH, Gabriele V, Kuniyoshi S et al., (1994) Occurrence of two molecular forms of human acid sphingomyelinase. *Biochem J 301:855-858*
- Furusho M, Dupree JL, Nave KA, Bansal R (2012) Fibroblast Growth Factor Receptor Signaling in Oligodendrocytes Regulates Myelin Sheath Thickness. *Journal of Neuroscience 32:6631-6641*
- Gandhi R, Laroni A, Weiner HL (2010) Role of the innate immune system in the pathogenesis of multiple sclerosis. *Journal of Neuroimmunology 221:7-14*
- Gatt S (1963) Enzymic Hydrolysis and Synthesis of Ceramides. *Journal of Biological Chemistry 238:3131-*
- Gol M, Ghorbanian D, Hassanzadeh S, Javan M, Mirnajafi-Zadeh J, Ghasemi-Kasman M (2017) Fingolimod enhances myelin repair of hippocampus in pentylentetrazol-induced kindling model. *European Journal of Pharmaceutical Sciences 96:72-83*
- Gold R. HH, Toyka KV (2000) Animal models for autoimmune demyelinating disorders of the nervous system. *Mol Med Today 6:88-91*
- Goldberg J, Clarner T, Beyer C, Kipp M (2015) Anatomical Distribution of Cuprizone-Induced Lesions in C57BL6 Mice. *Journal of Molecular Neuroscience 57:166-175*
- Goncalves DaSilva A, Yong VW (2009) Matrix Metalloproteinase-12 Deficiency Worsens Relapsing-Remitting Experimental Autoimmune Encephalomyelitis in Association with Cytokine and Chemokine Dysregulation. *The American Journal of Pathology 174:898-909*

- Gudi V (2010) Regional differences of molecular factors during demyelination and early remyelination in the CNS.
- Gudi V, Gingele S, Skripuletz T, Stangel M (2014) Glial response during cuprizone-induced de- and remyelination in the CNS: lessons learned. *Frontiers in Cellular Neuroscience* 8
- Gulbins E (2003) Regulation of death receptor signaling and apoptosis by ceramide. *Pharmacological Research* 47:393-399
- Gulbins E, Palmada M, Reichel M, Lüth A, Böhmer C, Amato D, Müller CP, Tischbirek CH, Groemer TW, Tabatabai G, Becker KA, Tripal P, Staedtler S, Ackermann TF, van Brederode J, Alzheimer C, Weller M, Lang UE, Kleuser B, Grassmé H, Kornhuber J (2013) Acid sphingomyelinase–ceramide system mediates effects of antidepressant drugs. *Nature Medicine* 19:934-938
- Gulbins E, Walter S, Becker KA, Halmer R, Liu Y, Reichel M, Edwards MJ, Müller CP, Fassbender K, Kornhuber J (2015) A central role for the acid sphingomyelinase/ceramide system in neurogenesis and major depression. *Journal of Neurochemistry* 134:183-192
- Haines JL, TerMinassian M, Bazyk A, Gusella JF, Kim DJ, Terwedow H, PericakVance MA, Rimmler JB, Haynes CS, Roses AD, Lee A, Shaner B, Menold M, Seboun E, Fitoussi RP, Gartioux C, Reyes C, Ribierre F, Gyapay G, Weissenbach J, Hauser SL, Goodkin DE, Lincoln R, Usuku K, GarciaMerino A, Gatto N, Young S, Oksenberg JR (1996) A complete genomic screen for multiple sclerosis underscores a role for the major histocompatibility complex. *Nature Genetics* 13:469-471
- Henderson APD, Barnett MH, Parratt JDE, Prineas JW (2009) Multiple sclerosis: Distribution of inflammatory cells in newly forming lesions. *Annals of Neurology* 66:739-753
- Howell OW, Rundle JL, Garg A, Komada M, Brophy PJ, Reynolds R (2010) Activated Microglia Mediate Axoglial Disruption That Contributes to Axonal Injury in Multiple Sclerosis. *Journal of Neuropathology & Experimental Neurology* 69:1017-1033
- Huan J, Culbertson N, Spencer L, Bartholomew R, Burrows GG, Chou YK, Bourdette D, Ziegler SF, Offner H, Vandenbark AA (2005) Decreased FOXP3 levels in multiple sclerosis patients. *Journal of Neuroscience Research* 81:45-52
- Jana A, Pahan K (2007) Oxidative stress kills human primary Oligodendrocytes via neutral sphingomyelinase: Implications for multiple sclerosis. *Journal of Neuroimmune Pharmacology* 2:184-193

- Jana A, Pahan K (2010) Sphingolipids in Multiple Sclerosis. *NeuroMolecular Medicine* 12:351-361
- Kanter JL, Narayana S, Ho PP, Catz I, Warren KG, Sobel RA, Steinman L, Robinson WH (2005) Lipid microarrays identify key mediators of autoimmune brain inflammation. *Nature Medicine* 12:138-143
- Paxinos and Franklin (2001) *The mouse brain in stereotaxic coordinates*. Academic press 2
- Kettenmann H, Hanisch UK, Noda M, Verkhratsky A (2011) *Physiology of Microglia*, Vol 91
- Kim HJ, Miron VE, Dukala D, Proia RL, Ludwin SK, Traka M, Antel JP, Soliven B (2011) Neurobiological effects of sphingosine 1-phosphate receptor modulation in the cuprizone model. *The FASEB Journal* 25:1509-1518
- Kim S, Steelman AJ, Zhang Y, Kinney HC, Li J (2012) Aberrant Upregulation of Astroglial Ceramide Potentiates Oligodendrocyte Injury. *Brain Pathology* 22:41-57
- Kipp M, Clarner T, Dang J, Copray S, Beyer C (2009) The cuprizone animal model: new insights into an old story. *Acta Neuropathologica* 118:723-736
- Kornhuber J, Tripal P, Reichel M, Muhle C, Rhein C, Muehlbacher M, Groemer TW, Gulbins E (2010) Functional Inhibitors of Acid Sphingomyelinase (FIASMA): A Novel Pharmacological Group of Drugs with Broad Clinical Applications. *Cellular Physiology and Biochemistry* 26:9-20
- Kuhlmann T, Lassmann H, Brück W (2008) Diagnosis of inflammatory demyelination in biopsy specimens: a practical approach. *Acta Neuropathologica* 115:275-287
- Kuhlmann T, Lingfeld G, Bitsch A, Schuchardt J, Bruck W (2002) Acute axonal damage in multiple sclerosis is most extensive in early disease stages and decreases over time. *Brain* 125:2202-2212
- Lassmann H, Bruck W, Lucchinetti C (2001) Heterogeneity of multiple sclerosis pathogenesis: implications for diagnosis and therapy. *Trends in Molecular Medicine* 7:115-121
- Liu, Y., X. Liu, W. Hao, Y. Decker, R. Schomburg, L. Fulop, M. Pasparakis, M. D. Menger, and K. Fassbender (2014). "IKK Deficiency in Myeloid Cells Ameliorates Alzheimer's Disease-Related Symptoms and Pathology", *Journal of Neuroscience*
- Lucchinetti C, Bruck W, Parisi J, Scheithauer B, Rodriguez M, Lassmann H (1999) A quantitative analysis of oligodendrocytes in multiple sclerosis lesions - A study of 113 cases. *Brain* 122:2279-2295

- Ludwin SK (1980) Chronic demyelination inhibits remyelination in the central nervous system. An analysis of contributing factors. *Lab Invest* 43:382-387
- Hiremath YS, G.W. Knapp, J.P.-Y. Ting, G.K. Matsushima (1998) Microglial macrophage accumulation during cuprizone-induced demyelination in C57BL/6 mice. *Journal of Neuroimmunology* 92 ;38–49
- Maceyka M, Spiegel S (2014) Sphingolipid metabolites in inflammatory disease. *Nature* 510:58-67
- Mason JL, Jones JJ, Taniike M, Morell P, Suzuki K, Matsushima GK (2000) Mature oligodendrocyte apoptosis precedes IGF-1 production and oligodendrocyte progenitor accumulation and differentiation during demyelination/remyelination. *Journal of Neuroscience Research* 61:251-262
- Matsushima GK, Morell P (2001) The neurotoxicant, cuprizone, as a model to study demyelination and remyelination in the central nervous system. *Brain Pathology* 11:107-116
- Merson TD, Binder MD, Kilpatrick TJ (2010) Role of Cytokines as Mediators and Regulators of Microglial Activity in Inflammatory Demyelination of the CNS. *NeuroMolecular Medicine* 12:99-132
- Messersmith DJ, Murtie JC, Le TQ, Frost EE, Armstrong RC (2000) Fibroblast growth factor 2 (FGF2) and FGF receptor expression in an experimental demyelinating disease with extensive remyelination. *Journal of Neuroscience Research* 62:241-256
- Mi S, Miller RH, Tang W, Lee X, Hu B, Wu W, Zhang Y, Shields CB, Zhang Y, Miklasz S, Shea D, Mason J, Franklin RJM, Ji B, Shao Z, Chédotal A, Bernard F, Roulois A, Xu J, Jung V, Pepinsky B (2009) Promotion of central nervous system remyelination by induced differentiation of oligodendrocyte precursor cells. *Annals of Neurology* 65:304-315
- Miron VE, Hall JA, Kennedy TE, Soliven B, Antel JP (2008a) Cyclical and Dose-Dependent Responses of Adult Human Mature Oligodendrocytes to Fingolimod. *The American Journal of Pathology* 173:1143-1152
- Miron VE, Jung CG, Kim HJ, Kennedy TE, Soliven B, Antel JP (2008b) FTY720 modulates human oligodendrocyte progenitor process extension and survival. *Annals of Neurology* 63:61-71
- Mohan H, Friese A, Albrecht S, Krumbholz M, Elliott CL, Arthur A, Menon R, Farina C, Junker A, Stadelmann C, Barnett SC, Huitinga I, Wekerle H, Hohlfeld R, Lassmann H, Kuhlmann T, Linington C, Meinl E (2014) Transcript profiling of different types of multiple sclerosis lesions yields FGF1 as a promoter of remyelination. *Acta Neuropathologica Communications* 2

- Mostert JP, Admiraal-Behloul F, Hoogduin JM, Luyendijk J, Heersema DJ, van Buchem MA, De Keyser J (2008) Effects of fluoxetine on disease activity in relapsing multiple sclerosis: a double-blind, placebo-controlled, exploratory study. *Journal of Neurology, Neurosurgery & Psychiatry* 79:1027-1031
- Mullen Thomas D, Hannun Yusuf A, Obeid Lina M (2012) Ceramide synthases at the centre of sphingolipid metabolism and biology. *Biochemical Journal* 441:789-802
- Ogretmen B, Hannun YA (2004) Biologically active sphingolipids in cancer pathogenesis and treatment. *Nature Reviews Cancer* 4:604-616
- Olitsky PK, Yager RH (1949) Experimental Disseminated Encephalomyelitis in White Mice. *Journal of Experimental Medicine* 90:213
- Pfeifenbring S, Nessler S, Wegner C, Stadelmann C, Bruck W (2015) Remyelination After Cuprizone-Induced Demyelination Is Accelerated in Juvenile Mice. *Journal of Neuropathology and Experimental Neurology* 74:756-766
- Phillip K. Peterson MT (2014) *Neuroinflammation and Neurodegeneration* ).
- Podbielska M, Krotkiewski H, Hogan EL (2012) Signaling and Regulatory Functions of Bioactive Sphingolipids as Therapeutic Targets in Multiple Sclerosis. *Neurochemical Research* 37:1154-1169
- Polman CH, Reingold SC, Banwell B, Clanet M, Cohen JA, Filippi M, Fujihara K, Havrdova E, Hutchinson M, Kappos L, Lublin FD, Montalban X, O'Connor P, Sandberg-Wollheim M, Thompson AJ, Waubant E, Weinshenker B, Wolinsky JS (2011) Diagnostic criteria for multiple sclerosis: 2010 Revisions to the McDonald criteria. *Annals of Neurology* 69:292-302
- Ponnusamy S, Meyers-Needham M, Senkal CE, Saddoughi SA, Sentelle D, Selvam SP, Salas A, Ogretmen B (2010) Sphingolipids and cancer: ceramide and sphingosine-1-phosphate in the regulation of cell death and drug resistance. *Future Oncology* 6:1603-1624
- Pugliatti M, Rosati G, Carton H, Riise T, Drulovic J, Vecsei L, Milanov I (2006) The epidemiology of multiple sclerosis in Europe. *European Journal of Neurology* 13:700-722
- Ransohoff RM, Kivisäkk P, Kidd G (2003) Three or more routes for leukocyte migration into the central nervous system. *Nature Reviews Immunology* 3:569-581
- Mayo clinic, research and education (2014) AskMayoExpert. What is multiple sclerosis? . Rochester, Minn
- Rőszer T (2015) Understanding the Mysterious M2 Macrophage through Activation Markers and Effector Mechanisms. *Mediators of Inflammation* 2015:1-16

- Sato F, Tanaka H, Hasanovic F, Tsunoda I (2011) Theiler's virus infection: Pathophysiology of demyelination and neurodegeneration. *Pathophysiology* 18:31-41
- Schuchman EH, Levrán O, Pereira LV, Desnick RJ (1992) Structural Organization and Complete Nucleotide-Sequence of the Gene Encoding Human Acid Sphingomyelinase (Smpd1). *Genomics* 12:197-205
- Skripuletz T, Hackstette D, Bauer K, Gudi V, Pul R, Voss E, Berger K, Kipp M, Baumgartner W, Stangel M (2012) Astrocytes regulate myelin clearance through recruitment of microglia during cuprizone-induced demyelination. *Brain* 136:147-167
- Sospedra M, Martin R (2005) Immunology of Multiple Sclerosis. *Annual Review of Immunology* 23:683-747
- Stoffel B, Bauer P, Nix M, Deres K, Stoffel W (1998) Ceramide-independent CD28 and TCR signaling but reduced IL-2 secretion in T cells of acid sphingomyelinase-deficient mice. *European Journal of Immunology* 28:874-880
- Syed A, Rizvi PKC (2011) *Clinical Neuroimmunology; Multiple Sclerosis and related disorders*
- Teichgräber V, Ulrich M, Endlich N, Riethmüller J, Wilker B, De Oliveira–Munding CC, van Heeckeren AM, Barr ML, von Kürthy G, Schmid KW, Weller M, Tümmler B, Lang F, Grassme H, Döring G, Gulbins E (2008) Ceramide accumulation mediates inflammation, cell death and infection susceptibility in cystic fibrosis. *Nature Medicine* 14:382-391
- Thannhauser S J RM (1940) Studies on animal lipids. XVI. the occurrence of sphingomyelin as a mixture of sphingomyelin fatty acid ester and free sphingomyelin, demonstrated by enzymatic hydrolysis and mild saponification.
- Rivers MD, et al., (1933) Observations on attempts to produce acute disseminated encephalomyelitis in monkeys
- Van Doorn R, Van Horssen J, Verzijl D, Witte M, Ronken E, Van Het Hof B, Lakeman K, Dijkstra CD, Van Der Valk P, Reijerkerk A, Alewijnse AE, Peters SLM, De Vries HE (2010) Sphingosine 1-phosphate receptor 1 and 3 are upregulated in multiple sclerosis lesions. *Glia*:n/a-n/a
- Wu YP, Mizugishi K, Bektas M, Sandhoff R, Proia RL (2008) Sphingosine kinase 1/S1P receptor signaling axis controls glial proliferation in mice with Sandhoff disease. *Human Molecular Genetics* 17:2257-2264
- Yu B, Zhou S, Wang Y, Qian T, Ding G, Ding F, Gu X (2012) miR-221 and miR-222 promote Schwann cell proliferation and migration by targeting LASS2 after sciatic nerve injury. *Journal of Cell Science* 125:2675-2683

- Yuan X-q, Qiu G, Liu X-j, Liu S, Wu Y, Wang X, Lu T (2012) Fluoxetine Promotes Remission in Acute Experimental Autoimmune Encephalomyelitis in Rats. *Neuroimmunomodulation* 19:201-208
- Zendedel A, Kashani IR, Azimzadeh M, Pasbakhsh P, Omid N, Golestani A, Beyer C, Clarner T (2016) Regulatory effect of triiodothyronine on brain myelination and astrogliosis after cuprizone-induced demyelination in mice. *Metabolic Brain Disease* 31:425-433

## 7 Publications

Based on the PhD experimental work and the results reached using the cuprizone animal model, the following manuscript was published:

- **Chami M**, Halmer R, Schnoeder L, Anne Becker K, Meier C, Fassbender K, et al. (2017) **Acid sphingomyelinase deficiency enhances myelin repair after acute and chronic demyelination**. PLoS ONE 12(6): e0178622. <https://doi.org/10.1371/journal.pone.0178622>

## 8 Acknowledgements

Foremost, I would like to thank my advisors PD. Dr. Silke Walter, Prof. Dr. Klaus Fassbender and Prof. Dr. Carola Meier for their outstanding support and guidance in accomplishing my thesis. In particular, PD. Dr. Silke Walter was a unique driving force from the beginning till the end of my project. I am heartily thankful to her, supervising my project with her enthusiasm and immense knowledge. I am grateful for their motivation, patience and all the valuable discussions we had during my PhD years. I want to thank also Dr. Yang Liu for his help in technical and theoretical problems.

I would like to thank my colleagues from AG Fassbender lab. Dr. Yann Decker, for all the discussions we had, the ideas we discussed and his supportive guidance with his knowledge and experience. Ms. Andrea Schottek, Ms. Inge Tomic and Ms. Rebecca Lancaster provided skillful technical support from the start till the completion of my thesis. I would like to thank also Ms. Laura Schnoeder for being a great neighbor and also for the great talks we had whether scientific or not, delivering by that a friendly and enjoyable atmosphere in our office. A special thanks also goes to Dr. Ramona Halmer, Dr. Sonja Gscheidle and Ms. Aniko Kasztner.

I would like to gratefully acknowledge the financial support for my thesis project from the German Research Foundation (DFG) and Novartis.

Lastly, I owe my gratitude to my family for their understanding and support during all these years.

## Figures

<b>Figure 1:</b> MRI abnormalities in relapsing–remitting multiple sclerosis. ....	11
<b>Figure 2:</b> Astrocytes orchestrate CNS inflammation. ....	16
<b>Figure 3:</b> Microglial activation as a continuous multistage process. ....	18
<b>Figure 4:</b> The sphingolipid signaling pathway .....	21
<b>Figure 5:</b> Experimental animal models .....	13
<b>Figure 6:</b> Weight measurments during chEAE.....	33
<b>Figure 7:</b> Representation of the corpus callosum. ....	39
<b>Figure 8:</b> Genetic Smpd1 deficiency prevents chEAE symtomp.....	47
<b>Figure 9:</b> Genetic Smpd1 deficiency inhibits lymphocyte infiltration to the spinal cord. ....	49
<b>Figure 10:</b> Smpd1 deficiency significantly decreases astrogliosis and microgliosis in chEAE.....	50
<b>Figure 11:</b> Pharmacological inhibition of Asm significantly decreases chEAE symptoms and demyelination.....	51
<b>Figure 12:</b> Asm inhibition by amitriptyline stops T cell infiltration.....	52
<b>Figure 13:</b> Brain sections with LFB and MBP.. ....	54
<b>Figure 14 :</b> Axonal damage analysis with IHC. ....	56
<b>Figure 15:</b> Effect of Asm <sup>-/-</sup> on astrogliosis and microgliois. ....	58
<b>Figure 16:</b> Brain sections stained for LFB and MBP.....	59
<b>Figure 17:</b> Stainings for APP and synaptophysin .....	61
<b>Figure 18:</b> Astrogliosis and microgliosis after amitriptyline treatment. ....	62

## Abbreviations

ASM	Acid sphingomyelinase
Asm	Acid sphingomyelinase (mouse)
Smpd1 -/-	Acid sphingomyelinase genetic knockout
APC	Antigen presenting cell
APP	Amyloid precursor protein
ATP	Adenosine triphosphate
ANOVA	One-way analysis of variance
BBB	Blood brain barrier
BDNF	Brain derived neurotrophic factor
CC	Corpus Callosum
CD-3	Cluster of differentiation-3
CD-4	Cluster of differentiation-4
CD-8	Cluster of differentiation-8
CFA	Complete Freud's Adjuvant
chEAE	chronic EAE
CNS	Central nervous system
dH <sub>2</sub> O	distilled water
DNA	Deoxyribonucleic acid
EAE	Experimental autoimmune encephalomyelitis
EBV	Epstein-Bar virus
FGF-1	Fibroblast growth factor-1
FGF-2	Fibroblast growth factor-2
FIASMA	Functional Inhibitor of Acid Sphingomyelinase
GDNF	Glial derived neurotrophic factor
GFAP	Glial fibrillary acidic protein
GPCRs	G-protein coupled receptors
h	Hour
H <sub>2</sub> O <sub>2</sub>	Hydrogen peroxide
HRP	Horse radish peroxide
Iba-1	Ionized calcium binding adapter-1
IgG	Immunoglobulin G
IgM	Immunoglobulin M
Il-1 $\beta$	Interleukin-1beta
Il-2	Interleukin-2
Il-4	Interleukin-4
Il-17	Interleukin-17
IFN $\gamma$	Interferon-g
IHC	Immunohistochemistry
i.p.	Intraperitoneally
i.v.	Intravenously

KO/ko	Knockout
M	Molar
MBP	Myelin Basic Protein
Mrc-1	Mannose receptor-1
MRI	Magnetic resonance imaging
MOG	Myelin Oligodendrocyte Glycoprotein
MS	Multiple sclerosis
NF-kb	Nuclear factor – kappa b
OPCs	Oligodendrocyte Precursor cells
Olig-2	Oligodendrocyte Transcription factor-2
LFA-1	Lymphocyte function antigen-1
LFB	Luxol Fast Blue
PA	Periodic Acid
PBS	Phosphate buffer with salt
PCR	Polymerase chain reaction
PFA	Paraformaldehyde
p.i.	Post immunization
PPMS	Primary progressive multiple sclerosis
RRMS	Relapsing remitting multiple sclerosis
RT	Room temperature
SD	Standard deviation
SEM	Standard error of the mean
SM	Sphingomyelin
Smpd-1	Sphingomyelin phosphodiesterase-1 gene
SphK-1	Sphingosine Kinase-1
SPMS	Secondary progressive multiple sclerosis
TBS	Tris buffer with salt
TBI	Traumatic brain injury
Treg	T cell regulatory
TGFb	Transforming growth factorb
TMEV	Theiler's Murine Encephalomyelitis virus
TNF- $\alpha$	Tumor necrosis factor-alpha
TLRs	Toll-like receptors
V	Ventricles
wks	Weeks
WT/wt	Wild-type